AD NUMBER

AD861267

NEW LIMITATION CHANGE

TO

Approved for public release, distribution unlimited

FROM

Distribution authorized to DoD only; Administrative/Operational Use; SEP 1969. Other requests shall be referred to Commanding General, U.S. Army Electronics Command, Attn: AMSEL-KL-IC, Fort Monmouth, NJ.

AUTHORITY

USAEC ltr, 12 Feb 1975

Research and Development Technical Report
ECOM-0301-F

AD861267

LINEAR INTEGRATED CIRCUITS (FIELD EFFECT RF AMPLIFIER/MIXER INTEGRATED CIRCUITS)

FINAL REPORT

By

R.H. DAWSON   S. KATZ

SEPTEMBER 1969

ECOM

UNITED STATES ARMY ELECTRONICS COMMAND · FORT MONMOUTH, N.J.

NOTICES

Disclaimers

Disposition

LINEAR INTEGRATED CIRCUITS (FIELD EFFECT RF AMPLIFIER/MIXER INTEGRATED CIRCUITS)

FINAL REPORT
8 APRIL 1968 TO 7 APRIL 1969

CONTRACT NO. DAAB07-68-C-0301
DA Project No. 1H6 62705 A 440, Task 02

Prepared By

R.H. DAWSON – S. KATZ

RCA ELECTRONIC COMPONENTS
SOMERVILLE, NEW JERSEY

For

U.S. ARMY ELECTRONICS COMMAND, FORT MONMOUTH, N.J.

SUMMARY

An integrated MOS RF amplifier-mixer circuit, capable of receiving FM signals in the 30-to 76-megahertz frequency range, was developed successfully. The front end IC essentially met or surpassed contract specifications on sensitivity, power gain, desensitization, and spurious response. The performance of the integrated-circuit compared favorably to results obtained from circuits using discrete devices.

The circuit, which consists of seven p-channel MOS enhancement devices fabricated on a common substrate, uses MOS dual-gate devices in both the direct-coupled RF amplifier and mixer stages. The MOS transistors necessary to bias these stages are included on the 30-by 40-mil pellet.

The RF amplifier-mixer IC was evaluated in a typical military FM receiver at 30 and 76 megahertz. The circuit exhibited an excellent sensitivity of 0.35 and 0.4 of a hard microvolt at 30 and 76 megahertz, respectively, for a 10-dB signal plus noise-to-noise ratio at the audio output. Power gain and dissipation was 34.0 dB and approximately 100 milliwatts, respectively, for a 9-volt supply at both 30 and 76 megahertz. Desensitization results were very good with interfering signal levels, removed by 10 percent from the desired channel frequency, of at least 122 dB above the reference level required to degrade the 10-dB signal plus noise-to-noise ratio to 6 dB. The integrated RF amplifier-mixer was operated in a varactor-tuned assembly, and performed well over the 63- to 76-megahertz band.

TABLE OF CONTENTS

iii

TABLE OF CONTENTS (Cont.)

LIST OF ILLUSTRATIONS

v

LIST OF ILLUSTRATIONS (Cont.)

LIST OF TABLES

LIST OF TABLES (Cont.)

SECTION I
INTRODUCTION

The goal of this program was the development of an MOS monolitnic integrated circuit having characteristics suitable for application as a building block in a wide variety of receiver front ends. The monolithic integrated circuit was to be incorporated in a voltage-tuned RF amplifier-mixer assembly capable of receiving signals in the frequency range of 30 to 76 megahertz, and producing an IF output in the range of 9 to 12 megahertz.

The capabilities of MOS field-effect devices for performing the functions of amplification and mixing, required in this assembly, were assessed during the investigation. The applicability of MOS field-effect devices for other purposes, such as biasing, coupling, and decoupling, also was determined. The ability to tune an MOS front-end IC with voltage-variable capacitors also was investigated.

It was the objective of this program that the following specifications should be met when the RF amplifier-mixer assembly was coupled to a crystal filter and an IF-audio system:

a. Sensitivity - An RF signal input of 0.6 microvolt modulated 1000 hertz at ±8 kilohertz deviation should produce a signal plus noise-to-noise ratio of not less than 10 dB when measured at a level of 50 milliwatts at the audio output into a 150-ohm resistive load.

b. Spurious Response - Spurious responses removed at least ±500 kilohertz from the desired frequency should be at least 80 dB below a 1.0-microvolt desired signal. There should be no more than five spurious responses within ±500 kilohertz which are less than 60 dB down from the 1.0-microvolt reference; there were to be no spurious signals less than 40 dB below the reference.

1

c. Cross Modulation and Desensitization - Cross-modulation and
    desensitization effects of interfering signals (modulated to 8
    kilohertz at 1000 hertz) on channels more than 1 megahertz from,
    and at a level of 60 dB above, the desired channel reference
    level (0.6 microvolt at 10-dB signal plus noise-to-noise ratio)
    should permit a signal plus noise-to-noise ratio of the desired
    signal of at least 6 dB.

Overall power gain of the RF amplifier-mixer assembly, designed for minimum
power dissipation, should be 34 dB.

A. DUAL-GATE MOS AS AN RF AMPLIFIER

Currently, the best approach to an RF MOS device is the dual-gate (tetrode) MOS transistor. A cross section of a p-channel unit is shown in Figure 1. This device incorporates two gates in series with a source-drain. Gate 1 is used for the signal in an RF amplifier stage, while gate 2 is at RF ground potential. The tetrode is essentially an integrated structure analogous to two MOS triodes in the classical cascode circuit. Extremely low feedback capacitance is exhibited, since the second gate acts as a ground shield for RF between the drain and first-gate electrodes, resulting in excellent RF stability. The device was designed to minimize parasitic capacitances, which result from gate overlap, by incorporating an oxide step at the edge of the channel. This close alignment is possible because the doped oxide, used as a diffusion source, assures automatic alignment of the resulting shallow diffusion with the undoped channel.

In addition, the center-point capacitance within the tetrode structure is minimized by using a very narrow diffusion. If the susceptance of this intermediate region (center point) becomes appreciable at high frequencies, as compared to the g_m associated with the second gate, the power gain and noise figure of the unit suffer.

The power gain of the device must be sufficient to overcome the noise level in the mixer stage and to meet the overall tuner power-gain requirement of 34 dB. The power gain of the RF stage is given by

$$G_p = \frac{|y_{21}|^2 \, \text{Re} \, Y_L}{|y_{22} + y_L|^2 \, \text{Re} \left(y_{11} - \dfrac{y_{12} \, y_{21}}{y_{22} + y_L} \right)} \quad \dots \dots \dots \dots \dots \quad (1)$$

3

DRAIN CONTACT

G2

OXIDE

G1

SOURCE CONTACT

P+

P

P

P

P

P+

N-TYPE SILICON SUBSTRATE

INTERMEDIATE REGION

DRAIN

SOURCE
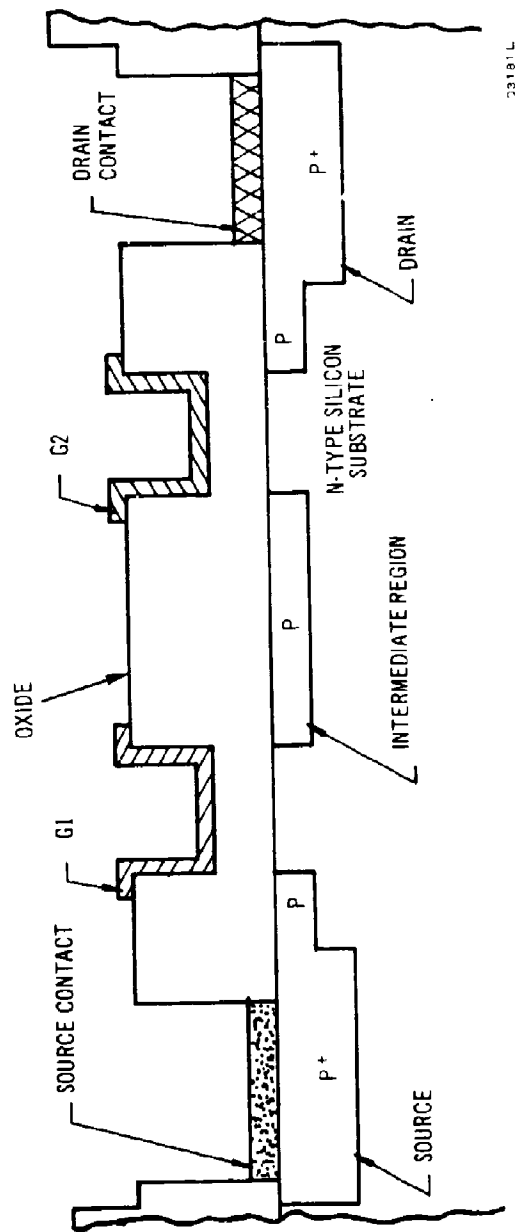
Figure 1. Cross Section of MOS Dual-Gate Transistor

4

where

y_{11} = input admittance of the tetrode

y_{22} = output admittance of the tetrode

y_{12} = input transfer admittance of the tetrode

y_{21} = output transfer admittance of the tetrode

for the frequencies of interest $\left| y_{21} \right| \approx g_m$, device transconductance.

The noise figure of the RF amplifier is mainly responsible for determining the sensitivity of the receiver.

Cross-modulation distortion occurs when third-order and higher-order signal nonlinearities are present. The modulation of an undesired carrier frequency (interfering signal) transfers to the desired carrier frequency. Cross-modulation distortion of the dual-gate MOS structure is quite low.

The selectivity of the RF amplifier stage is important in rejecting adjacent-channel signals. Good selectivity requires high-Q tank circuits, which are dependent upon device impedance. The high input and output impedances of the tetrode result in highly selective tank circuits, thereby minimizing cross-modulation distortion, desensitization, and spurious responses.

A comparative analysis of the dual-gate MOS transistor and the triode MOS transistor shows that the dual-gate RF amplifier is stable over a wider frequency range than the MOS triode. Further, the voltage gain is inherently much higher in the dual-gate structure than it is in the triode for equivalent stability factors. In the present application of the dual-gate MOS transistor from 30 to 76 megahertz, a certain degree of mismatch must be used at the low-frequency end to obtain adequate stability. Since mismatch is not necessary at the higher frequencies, the gain is considerably greater than that obtainable with a analogous MOS triode.

The stability of the RF amplifier stage is analyzed through the use of Stern's stability factor, K, which is given by

$$K = \frac{\left| y_{12}\, y_{21} \right|}{2\, g_{11}\, g_{22}\, (1 + m_1)(1 + m_2) - \mathrm{Re}\,(y_{12}\, y_{21})} \quad \cdots \cdots \cdots (2)$$

5

where

y_{12} = input transfer admittance of the tetrode

y_{21} = output transfer admittance of the tetrode

g_{11} = input parallel conductance of the tetrode

g_{22} = output parallel conductance of the tetrode

$m_1 \equiv \dfrac{G_s}{g_{11}}$ and G_s = source conductance

$m_2 \equiv \dfrac{G_L}{g_{22}}$ and G_L = load conductance

The RF amplifier is stable if $0 < K < 1$.

B. P-CHANNEL DUAL-GATE MOS TRANSISTORS

The choice of a p-channel transistor for the RF amplifier-mixer circuit
was primarily based on two factors: p-channel enhancement transistor could be
direct coupled easily, and the 1-to 2-volt threshold values were convenient
for threshold biasing schemes for use with a low value (9 volt) supply voltage.
In addition, it has been observed in our laboratories that the equivalent noise
current in p-channel transistors is lower than that in similar geometry (0.2-
mil channel length) n-channel transistors over a midband of frequencies from
500 kilohertz to 100 megahertz. Independent, detailed experimental and
theoretical work that substantiates the observation of lower equivalent p-chan-
nel noise current over the same frequency band has been done by H. E. Halladay
in his doctoral thesis, Noise in MOS Field Effect Transistors, University of
Minnesota, August 1967. Halladay's thesis indicates that the excess noise
current above thermal noise from the channel resistance is a factor of 4 to 5
for n-channel transistors compared to 1.5 to 2 for p-channel transistors. The
difference in excess noise factors was attributed to a combination of two
factors: lower p-channel mobility, and reduced scattering from fluctuating
positive oxide charge scattering centers for p-channel transistors. While the
theory developed appears to account for the difference in excess noise levels
between p- and n-channel devices, it has not been substantiated fully. In
agreement with these observations, excellent RF sensitivity from 30 to 76 mega-

6

hertz was measured in both the preliminary breadboard circuits and the final integrated p-channel circuits.

During the early portion of the program, a process was developed for fabricating high-frequency, p-channel transistors. This process provided for the accurate definition of 0.2-mil channels as well as for the location of oxide steps that are aligned automatically to the channel edges. These oxide steps reduce feedback capacitance a considerable degree; thereby improving amplifier RF stability.

At the outset of the program, several photomasks were available to fabricate high-frequency, p-channel transistors for the purpose of breadboarding the integrated circuit components. These masks had been used previously to fabricate high-frequency, n-channel depletion transistors by a process similar to the one currently used to fabricate p-channel transistors. The n-channel process is described in Final Report ECOM-00001-F, Transistor, Field-Effect, Insulator Gate, 100 MC Amplifier, March 1966. The various photomasks available, as specified by the channel dimensions, were 0.2 by 20 mil, 0.2 by 40 mil, and 0.2 by 70 mil. The choice was made to fabricate the 0.2- by 40-mil structure as a test vehicle.

A photomicrograph of the 40-mil dual-gate transistor structure is shown in Figure 2. The decision to use the 0.2- by 40-mil structure was made on the basis of a compromise between input impedance levels and power dissipation. The smallest structure would have the lowest power dissipation, but impedance levels would be difficult to match with varactor-tuned circuits that have somewhat lower Q's than air-gap tuning capacitors. The largest unit would have relatively low impedance levels, but power dissipation would run high. The 0.2- by 40-mil transistors that were fabricated and used for the breadboard circuit had power dissipations of about 65 milliwatts and impedance levels that were low enough so that matching was not a problem. The devices exhibited a transconductance between gate 1 and drain of 3400 micromhos at a drain current of 7 milliamperes, for $V_{G1S} = -5$ volts, $V_{G2S} = V_{DD} = -9$ volts (where V_{G1S} is gate 1-to-source voltage, V_{G2S} is gate 2-to-source voltage, and V_{DD} is the drain supply voltage). Typical threshold voltages of -1.7 volts were measured.

7
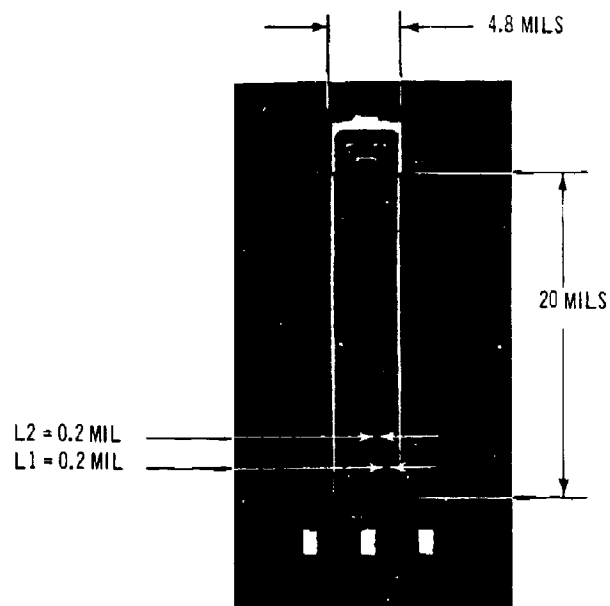
Figure 2. Photomicrograph of the 40-by 0.2-Mil Dual-Gate MOS Folded Structure

C. DUAL-GATE MOS AS A MIXER

The dual-gate MOS provides the best capability in meeting the device requirements for a mixer stage of an FM receiver. The mixer should exhibit high conversion gain and good stability with a minimum of spurious responses, RF oscillator radiation, and cross-modulation distortion.

Electrical instabilities (oscillations) normally are not a problem in a mixer if the RF and IF signals are relatively far apart in frequency. Under these conditions, the output of the mixer circuit presents a low impedance to the RF signal, and the input of the mixer presents a low impedance to the IF signal. Oscillation at either frequency, therefore, is unlikely to occur. The tetrode, with its extremely low feedback capacitance, would be even less likely to oscillate in a mixer stage.

Spurious responses are generated when harmonics of the RF oscillator signal beat with harmonics of the incoming signal to form a signal at intermediate frequencies (IF). The most severe spurious response in most FM tuners is the IF/2 response, which occurs at a frequency 5.35 megahertz above the frequency of the desired signal. Spurious responses are increased when mixing occurs in a nonlinear region of device operation. Because the dual-gate device ideally does not require use of the nonlinear region of its operating characteristic for mixing action, as does an MOS triode, cross-modulation distortion and spurious responses are reduced. Due to the low levels of undesired signals, the RF oscillator injection level can be increased to optimize conversion gain, the ratio of IF power output to RF power input. Some compromise also must be made, however, between conversion gain and desensitization.

Separation of the RF signal from the RF oscillator signal yields a large degree of isolation, due to the very low gate-to-gate capacitance. This isolation reduces RF oscillator radiation toward the antenna and pulling with strong RF signals, i.e., variations in amplitude of RF signals that change the frequency of the RF oscillator.

In devices that have a single input electrode, mixing operation occurs because of the nonlinearity of the device. The transfer function for such a device can be expressed as a power series in which the quadratic terms indicate

the desired mixing function and the other terms contribute cross-modulation and intermodulation products.

Although the dual-gate MOS structure can be used as a single-input device, the advantage of this transistor lies in the use of both gates. The schematic diagram of the dual-gate MOS transistor (tetrode) is shown in Figure 3.

The total AC drain current of the mixer can be expressed as follows

$$i_d = g_{m1} v_{g1} + g_{m2} v_{g2} \quad \cdots \cdots \cdots \cdots \cdots \cdots \quad (3)$$

where g_{m1} is the transconductance between gate 1 and drain and g_{m2} is the transconductance between gate 2 and drain. Typical plots for g_{m1} and g_{m2} of the high-frequency p-channel enhancement unit are shown in Figure 4 and Figure 5. At a specific DC biasing, the transconductance can be approximated by a straight line in general parameters as follows

$$g_{m1} = a_1 + b_1 v_{g2} \quad \cdots \cdots \cdots \cdots \cdots \cdots \cdots \quad (4)$$

$$g_{m2} = a_2 + b_2 v_{g1} \quad \cdots \cdots \cdots \cdots \cdots \cdots \cdots \quad (5)$$

The variation of transconductance as a function of one gate voltage with the other gate voltage constant is shown in Figure 6. The transconductance, g_{m1}, exhibits a fairly large, linear range with respect to gate 2 voltage for $V_{G1S} = -6$ volts. Substituting Eq. (4) and Eq. (5) into Eq. (3), the drain current becomes

$$i_d = a_1 v_{g1} + a_2 v_{g2} + (b_1 + b_2) v_{g1} v_{g2} \quad \cdots \cdots \cdots \cdots \quad (6)$$

Let the voltages on gate 1 and gate 2 be defined as

$$v_{g1} = E_1 \sin \omega_1 t \quad \cdots \cdots \cdots \cdots \cdots \cdots \cdots \cdots \quad (7a)$$

$$v_{g2} = E_2 \sin \omega_2 t \quad \cdots \cdots \cdots \cdots \cdots \cdots \cdots \cdots \quad (7b)$$
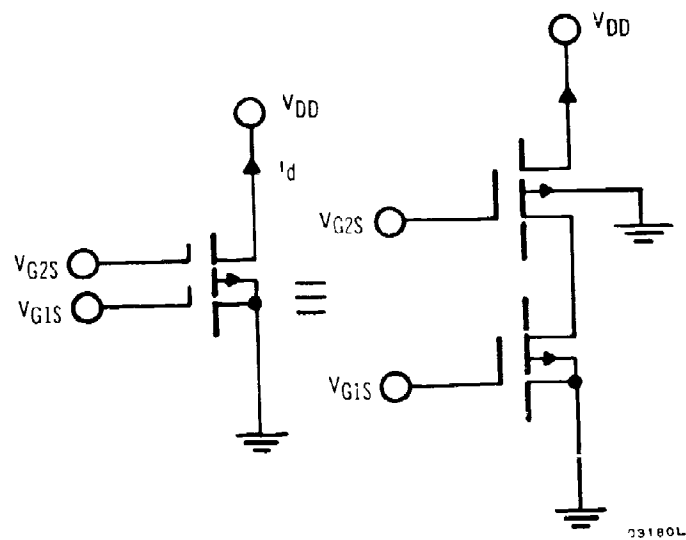
Figure 3. Schematic Representation of a Tetrode

11
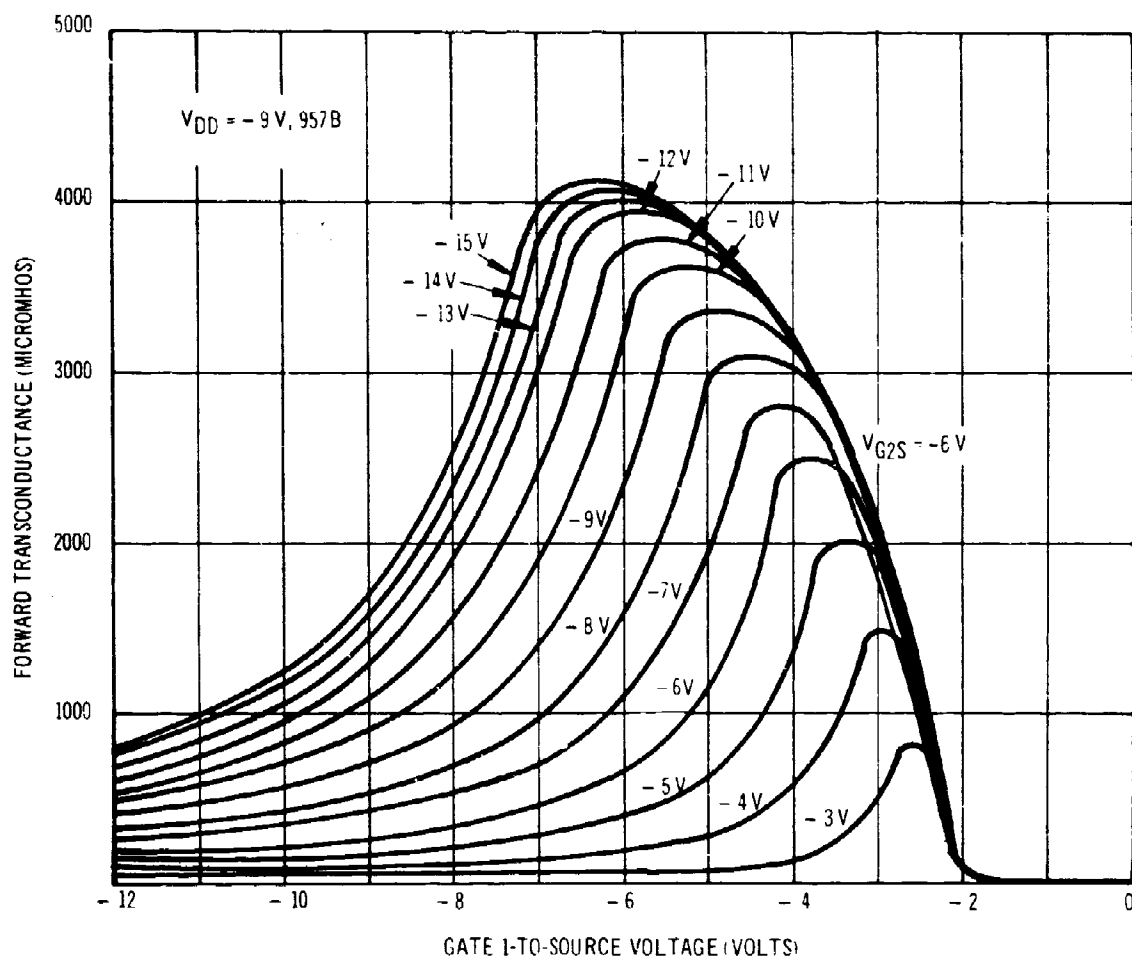
Figure 4. Gate 1-to-Drain Forward Transconductance of a Dual-Gate MOS Transistor as a Function of
Gate 1-to-Source Voltage for Values of Gate 2-to-Source Voltage

12
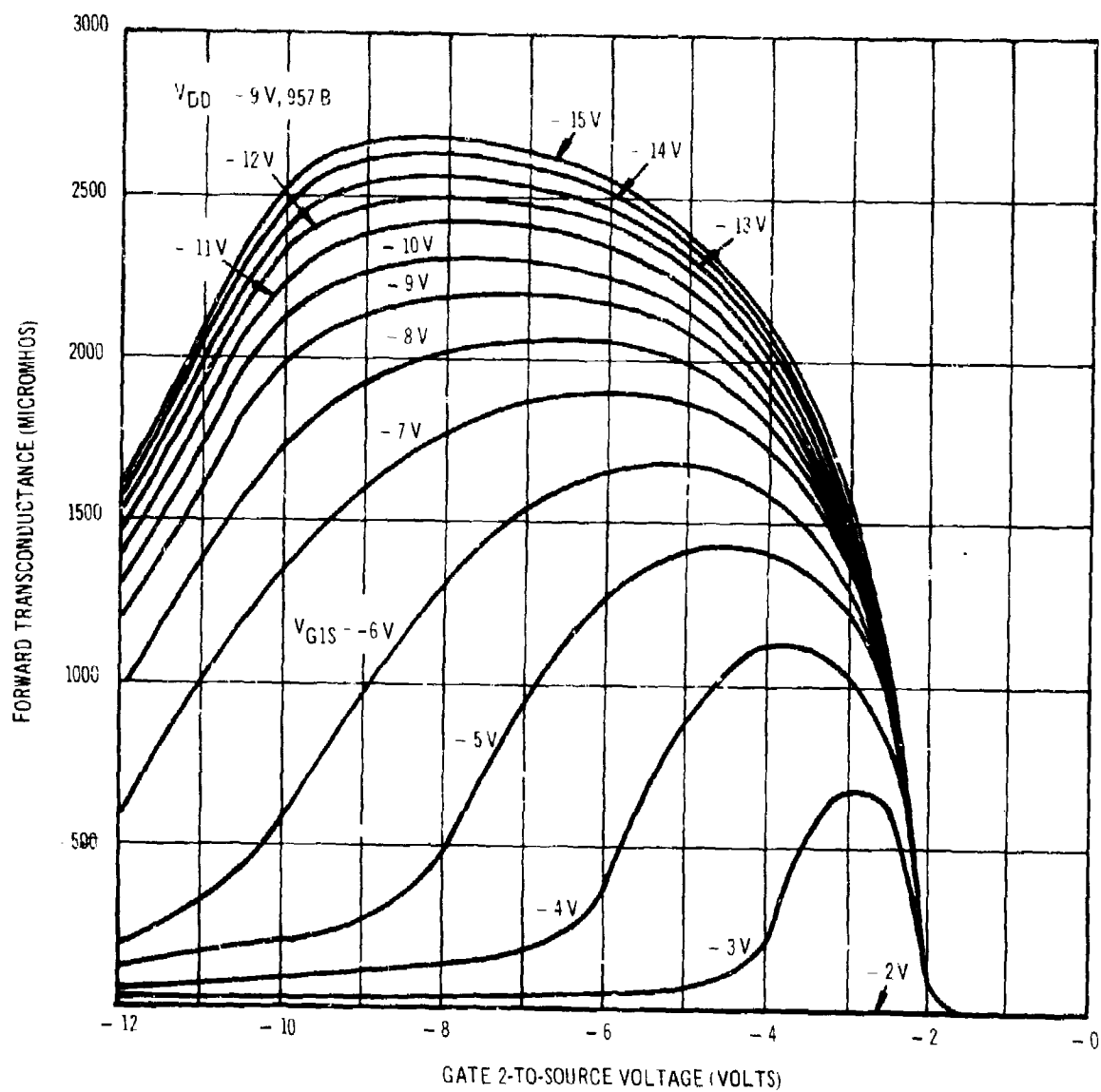
Figure 5. Gate 2-to-Drain Forward Transconductance as a Function of Gate 2 Voltage for
Values of Gate 1-to-Source Voltage

13
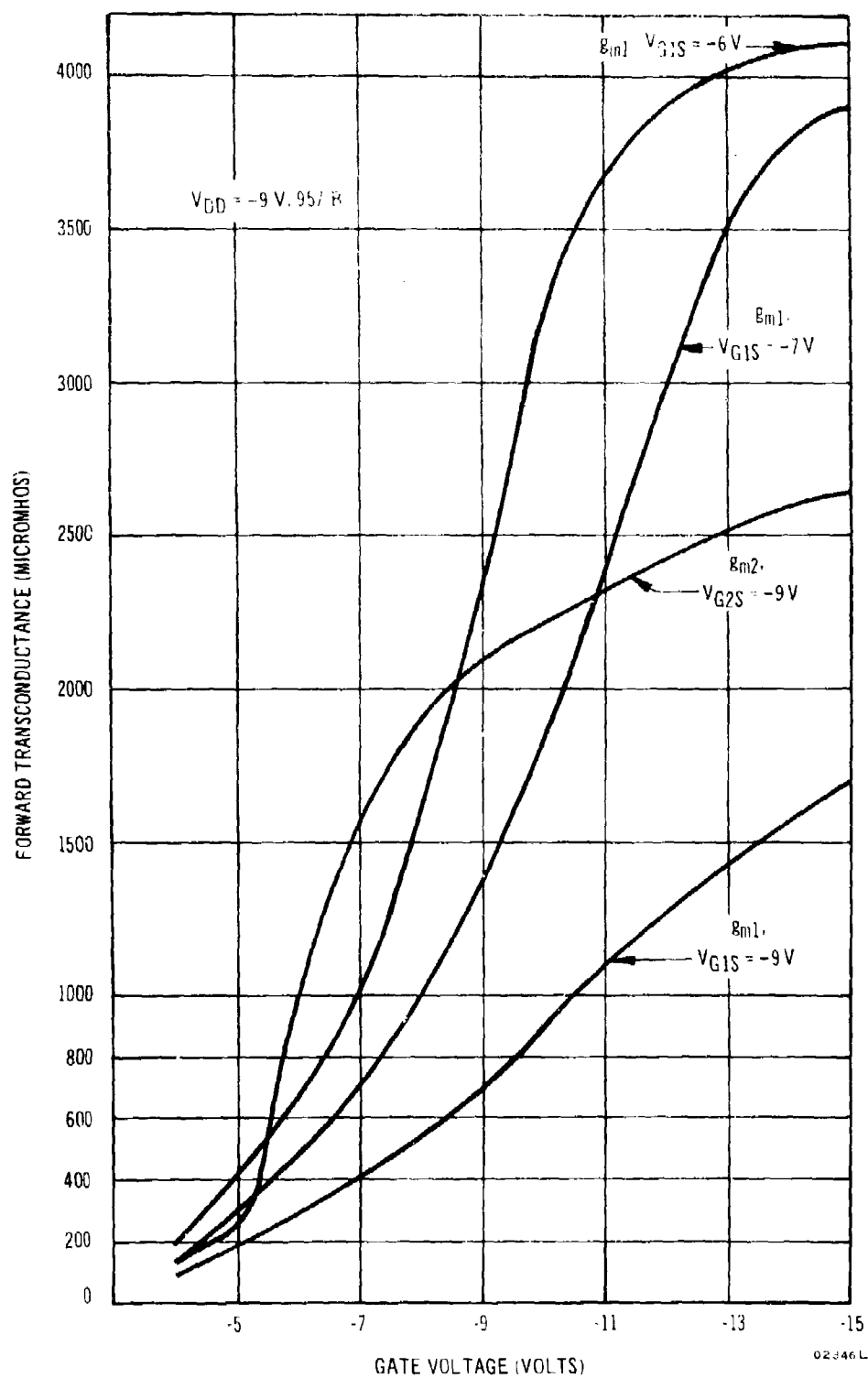
Figure 6. Gate-to-Drain Forward Transconductance as a Function of One
Gate Voltage for a Constant Other Gate-to-Source Voltage

14

Then the mixing term of the drain current can be expressed as follows

$$i_{dm} = (b_1 + b_2) \, E_1 \, E_2 \left[\frac{1}{2}\cos(\omega_1 + \omega_2)t + \frac{1}{2}\cos(\omega_2 - \omega_1)t \right]$$

In this equation, the intermediate frequency term is defined as

$$i_{dm} \quad \frac{1}{2}(b_1 + b_2) \, E_1 \, E_2 \, \cos(\omega_2 - \omega_1)t$$

If the local oscillator injection is at gate 2, and the signal is applied at gate 1, then $E_1 = E_s$, $\omega_1 = \omega_s$, $E_2 = E_{LO}$, $\omega_2 = \omega_{LO}$, and the conversion transconductance g_{mc} is

$$g_{mc} \equiv \left| \frac{i_{dm}}{E_s} \right| = \frac{1}{2}(b_1 + b_2) \, E_{LO} \quad \cdots \cdots \cdots \cdots \cdots \quad (8)$$

It is observed from Eq. (8) that the conversion transconductance at a specified bias condition is proportional to the sum of the slopes of g_{m1} and g_{m2}, or the variation of transconductance with respect to the gate voltage.

D. MOS BIASING AND LEVEL SHIFTING NETWORKS

In addition to MOS transistors functioning as active elements, MOS structures can also be used to form biasing networks. Figure 7 shows two biasing configurations that can be used for MOS integrated circuits. The conventional load bias for p-channel devices is shown in A, Figure 7. Voltage V_S divides in proportion to the resistive division. Equal division (shown as an example) occurs when equal-size MOS units are used. Threshold load bias, for enhancement units, is shown in B, Figure 7. A low-conducting MOS is used at the top of the string, which starves the lower MOS units. The lower units, therefore, operate at very nearly their threshold voltage. Various integrals of threshold voltage are obtained at the taps, with the restriction that current is not drawn at these taps. This restriction is satisfied, since MOS gates do not draw current. Voltages at these taps are essentially independent of power supply variations.

15

A. CONVENTIONAL LOAD BIAS
(EQUAL SIZE MOS UNITS)

B. THRESHOLD LOAD BIAS
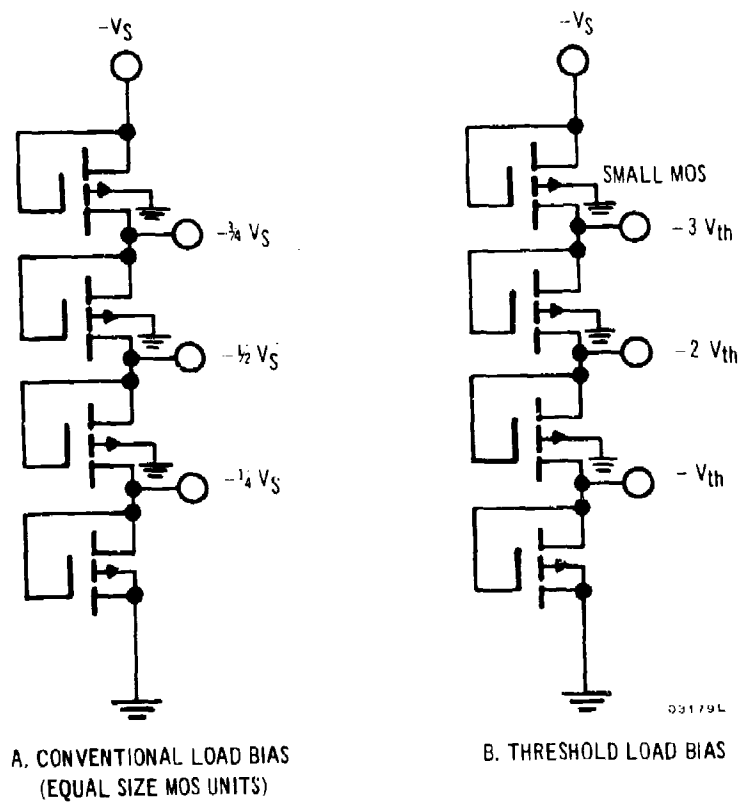
Figure 7. MOS Biasing Networks

16

Enhancement MOS devices can also be incorporated in an integrated circuit for level-shifting DC voltages. One approach is the unity-gain source-follower level shifter for p-channel units shown in Figure 8. A source-follower with equal-size transistors, for example, drops the level by V, which is the DC voltage on the lower gate shown in Figure 8.

In addition to dependence upon the geometry and physical properties of the transistor, threshold voltage is also a function of the potential difference between the source and the substrate on which the device is fabricated. Substrate bias normally is a reverse bias across the pn junction between the source and the substrate. As the reverse substrate bias is increased, the threshold voltage increases. The integrated bias and level-shifting circuit will deviate from ideal conditions, because each device does not exhibit exactly the same V_T. The effect is much less pronounced, however, with p-channel MOS units, which have lower doped substrates, than with n-channel devices.

E. PRELIMINARY DIRECT-COUPLED RF AMPLIFIER-MIXER CIRCUITS

Several direct-coupled RF amplifier-mixer circuits were investigated. Two such direct-coupled RF amplifier-mixer circuits, with the local-oscillator signal injected at gate 1 and gate 2, shown in Figures 9 and 10, respectively, were breadboarded and tested. The circuits incorporate dual-gate p-channel enhancement devices (Q1 and Q2), MOS threshold bias (Q3 through Q5), reactive coupling components, a dummy antenna, and a single 9-volt supply. The bias network was breadboarded with semi-integrated, low-frequency, enhancement p-channel transistors, four to a package.

The threshold-bias technique is used to provide good DC stability of tetrode Q1. The source-to-gate potential of Q1 is essentially $2V_T$ and is independent of supply voltage. The drain current of transistor Q1 is $K_1 V_T^2$ and is independent of supply voltage. Enhancement MOS devices permit direct coupling of the RF amplifier and mixer stages.

As shown in Figures 9 and 10, the RF input gate of MOS tetrode Q1 is biased at $V_S - 2V_T$, while gate 2 is at zero potential. If V_S is greater than $V_S > 3V_T$, both triodes of the same geometry that make up tetrode Q1 will be biased in
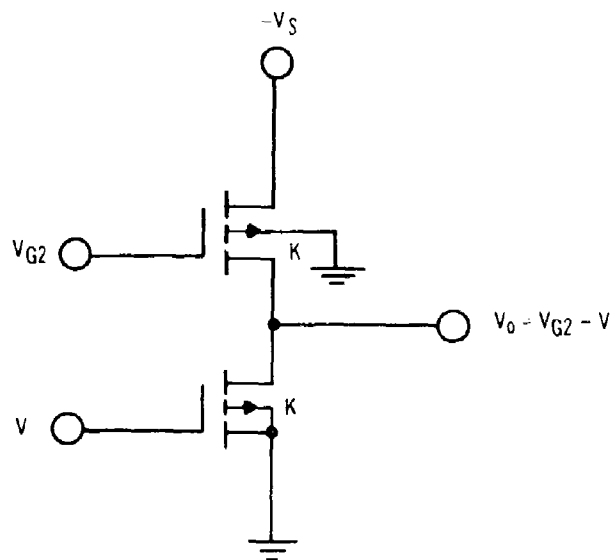
Figure 8. Source Follower with Equal Size Transistor Level Shifter

03178L

18
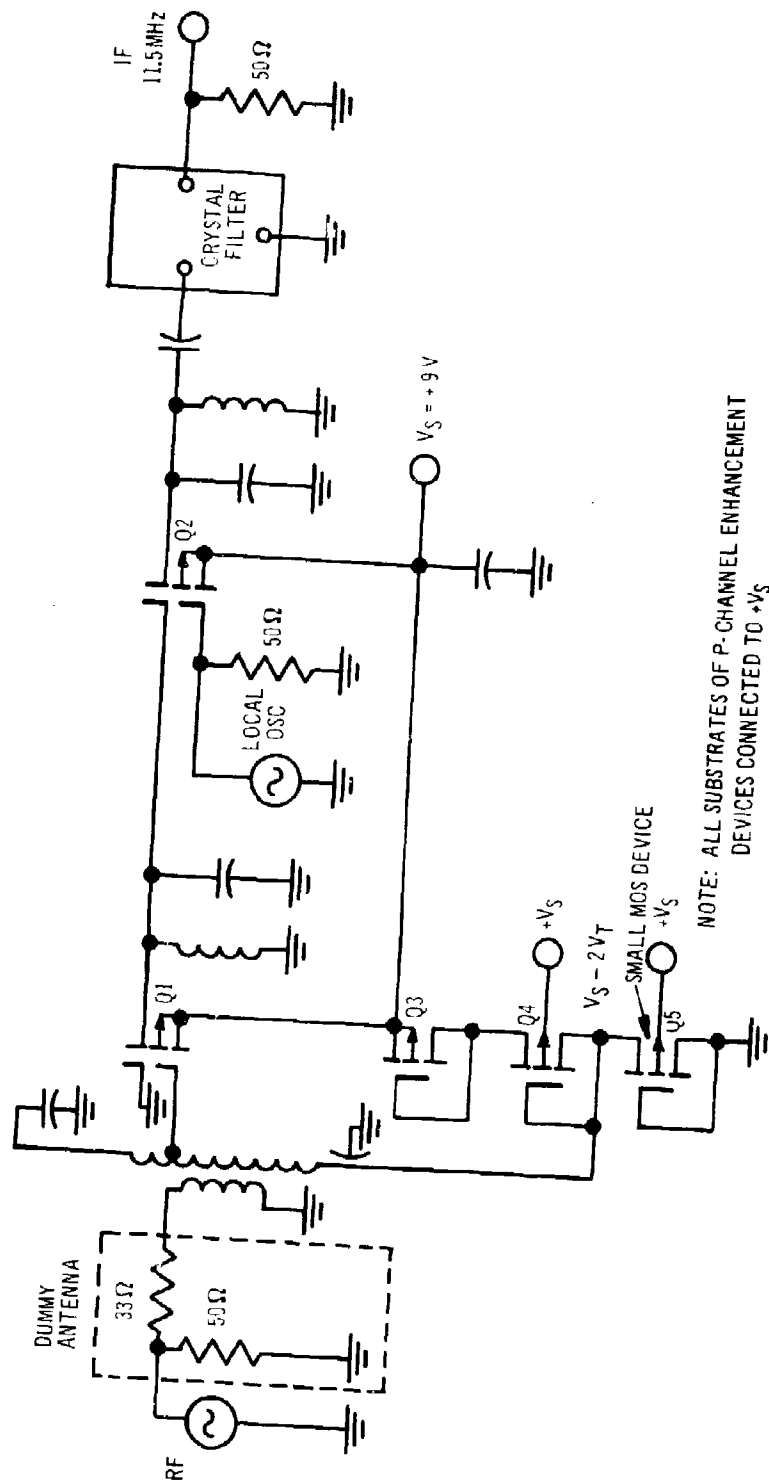
Figure 9. Direct-Coupled RF Amplifier-Mixer Circuit with Local Oscillator Injection at Gate 1

NOTE: ALL SUBSTRATES OF P-CHANNEL ENHANCEMENT DEVICES CONNECTED TO +V_S

02475L

19
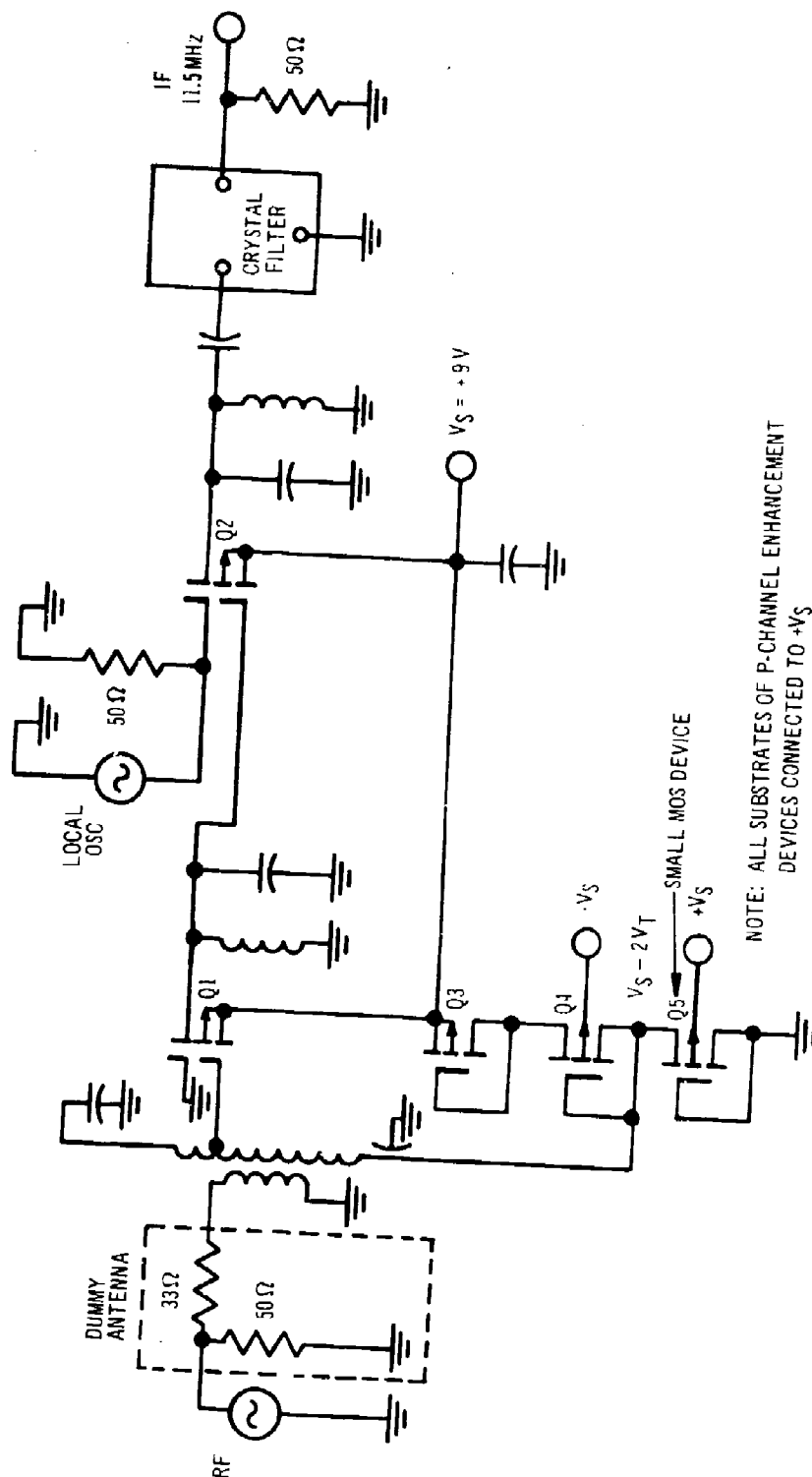
Figure 10. Direct-Coupled RF Amplifier-Mixer Circuit with Local Oscillator Injection at Gate 2

NOTE: ALL SUBSTRATES OF P-CHANNEL ENHANCEMENT DEVICES CONNECTED TO +V_S

20

the pinch-off region. These bias conditions ensure that RF amplifier transistor Q1 operates in the region of high RF gain. The single-tuned circuit at the RF amplifier-mixer interstage provides selectivity, but no matching. Consequently, the input resistance of the mixer was designed to be nearly equal to the output resistance of the RF amplifier, and the power transfer from the RF amplifier to the mixer is almost optimum.

With the RF oscillator biased at ground potential, gates 1 and 2 of tetrode Q2 in the mixer stage are both at zero potential. The triode associated with gate 1 is below the pinch-off region, while the unit with gate 2 is in the pinch-off condition (for triodes of the same geometry). The mixer output was matched for maximum power transfer to a crystal bandpass filter with a nominal impedance of 50 ohms through a matching network.

The power gains exhibited by the direct-coupled circuits of Figures 9 and 10, not including losses in the dummy antenna or the crystal filter, were 31.0 dB and 25.5 dB with a 3-volt-RMS, 41.5-megahertz local oscillator signal injected at gate 1 and gate 2, respectively, of mixer Q2. The quiescent power dissipation for both circuits was approximately 175 milliwatts with a 9-volt power supply.

Another alternative for mixing is the injection of the local oscillator at the source of device Q2, for either RF amplifier-mixer of Figures 9 and 10. For the circuit in discrete form, the source and substrate of transistor Q2 are connected so that the diode between the source and the substrate would never be forward biased. This connection cannot be made in the integrated circuit, however, because the common substrate of the p-channel unit is connected to $+V_S$ for our present circuit configuration.

If the substrate and source are biased at the same DC level, then the diode between the source and the substrate will conduct for the positive portion of the local oscillator signal at the source.

One possible approach for source injection is to use two power supplies. The source could be biased at lower voltage than the peak oscillator swing such that the diode between the source and the substrate will never conduct

21

(even at the highest level of local oscillator injection). Source injection, however, increases the overall power dissipation of the system since the local oscillator is required to drive the low impedance input of device Q2. In addition, the reverse-biased diode between the source and substrate acts as a varactor diode, which could increase the amount of distortion. For these reasons, the source injection of the local oscillator was not pursued.

F. AC COUPLED AND DC LEVEL-SHIFTING RF AMPLIFIER-MIXER CIRCUIT

Although the DC coupled RF amplifier-mixer circuit is very attractive for integration because of its simplicity, it does not permit the mixer stage to be biased in its optimum region (as seen from the curves of Figure 4). The AC coupled circuit depicted in Figure 11 permits the dual-gate mixer device to be biased where the variation in g_{m1} transconductance is largest and most linear. Again, the threshold-bias technique and a single supply were used. Gate 1 of transistor Q2 is biased at approximately $V_S - 3V_T$, while the local oscillator is injected at gate 2 which is biased at ground potential. The g_{m2} transconductance curves of Figure 5 indicate that there would be no advantage to injecting the local oscillator at gate 1 in an AC coupled approach.

An overall gain of 35 dB was measured at 30 megahertz with a 9-volt supply and a 3-volt-RMS local oscillator injected at gate 2. In addition, the quiescent power dissipation decreases from 175 milliwatts for the DC coupled circuit to 150 milliwatts for the AC circuit of Figure 11. As predicted, the gain with a local oscillator injected at gate 1 did not exhibit any improvement over the direct circuit.

Although the circuit of Figure 11 results in higher gain with less standby power dissipation than the circuits of Figures 9 and 10, it requires an external capacitor and pin connection at the amplifier-mixer interstage. The circuit of Figure 12 was designed and permits the dual-gate mixer device, Q2, to be biased in a region similar to that of the AC coupled circuit. The bias for gate 1 of Q2 is obtained with the level-shifting source-follower stage, Q3 and Q4. The DC level-shifting scheme was to replace the external capacitor and pin connection of Figure 11 while maintaining similar circuit performance.

22

Figure 11. AC-Coupled RF Amplifier-Mixer Circuit

NOTE: ALL SUBSTRATES OF P-CHANNEL ENHANCEMENT
DEVICES CONNECTED TO +V$_S$
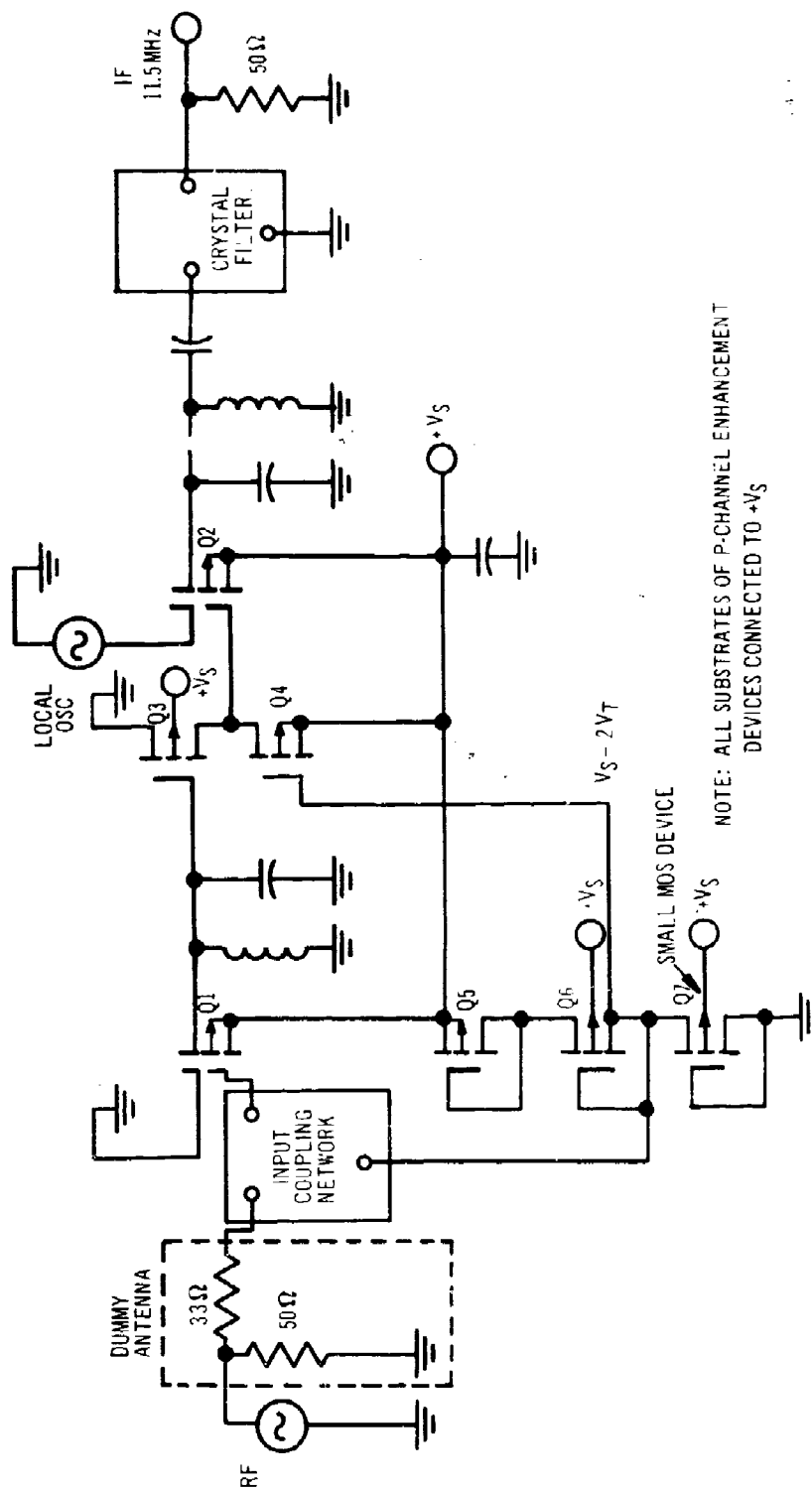
Figure 12. DC-Level-Shifting RF Amplifier-Mixer Circuit

NOTE: ALL SUBSTRATES OF P-CHANNEL ENHANCEMENT DEVICES CONNECTED TO +V_S

24

The circuit of Figure 12 was breadboarded; ho, er, it exhibited poor gain. The major problem was that the gain of the source follower, which ideally is unity at low frequencies, decreased rapidly at the frequencies of interest, i.e., 30 to 76 megahertz. Consequently, the DC level-shifting approach is not suited for use in the frequency range of interest.

G. SYSTEM PERFORMANCE OF PRELIMINARY DIRECT AND AC COUPLED RF AMPLIFIER-MIXER CIRCUITS AT 30 MEGAHERTZ

The overall system performance was evaluated for both preliminary direct-coupled RF amplifier-mixer circuits of Figures 9 and 10 in a typical military FM receiver at a frequency of 30 megahertz. Sensitivity, spurious response, cross-modulation distortion, and desensitization were measured. All measurements were taken for a 9-volt supply and 3-volt-RMS local oscillator signal.

The audio output signal plus noise-to-noise ratio, (S+N)/N, as a function of RF signal input (modulated by 1000 hertz at ±8 kilohertz deviation) is given in Table I. Sensitivities (for a 10 dB output (S+N)/N ratio) are 0.33 and 0.35 hard microvolt for local oscillator signal injected at gate 2 and gate 1, respectively. These measurements, which include loss in the dummy antenna, exceed the specification requirement of 0.6-microvolt RF signal for a 10-dB signal plus noise-to-noise ratio.

The results of cross-modulation-distortion and desensitization tests at 30 megahertz for both circuits are given in Table II. The amount of inter-fering-signal level required to degrade the 10-dB audio output signal plus noise-to-noise ratio to 6 dB is listed for several channels at least 1 mega-hertz from the desired channel. The results, which were similar for both modes of local oscillator injection, exceed the requirement of 60 dB of interfering signal above the desired reference level.

Table III provides a comparison of spurious response at 30 megahertz for both local oscillator injection schemes. The first step of the method used was to measure the quieting produced by a 1.0-hard-microvolt, 30-megahertz, unmodulated input signal. Using this level as a reference, the input then was swep⁻ in frequency, and the signal levels at which quieting was equal to that produced by the 1.0-hard-microvolt signal were recorded at the spurious-response

25

TABLE I. AUDIO OUTPUT (S+N)/N VERSUS RF SIGNAL INPUT
AT 30 MEGAHERTZ FOR DIRECT-COUPLED CIRCUITS

RF Signal (hard μV)	Audio Output (S+N)/N (dB)	
	Local Oscillator Injection at Gate 1	Local Oscillator Injection at Gate 2
1.00	25.0	26.0
0.50	16.0	17.0
0.40	12.0	13.0
0.35*	10.0	10.5
0.33*		10.0

*Sensitivity relative to front end specification
set forth in technical guidelines (see Section I).

TABLE II. DESENSITIZATION AT 30 MEGAHERTZ
FOR DIRECT-COUPLED CIRCUITS

	Signal Magnitude Above Reference Level	
Interfering-Signal Frequency (MHz)	Local Oscillator Injection at Gate 1, Ref. = 0.35 µV (dB)	Local Oscillator Injection at Gate 2, Ref. = 0.33 µV (dB)
27.0	127.2	126.4
29.0	108.6	107.4
31.0	105.6	106.8
33.0	125.2	124.4

TABLE III. SPURIOUS RESPONSE AT 30 MEGAHERTZ
FOR DIRECT-COUPLED CIRCUITS

Spurious Frequency (MHz)	Spurious Order	Magnitude Above 1-µV Reference Level	
		Local Oscillator Injection at Gate 1 (dB)	Local Oscillator Injection at Gate 2 (dB)
53.000	2	77.5	80.2
15.000	3	97.0	97.0
26.500	3	117.4	90.6
17.666	4	115.3	113.0
35.750	4	107.5	103.5
23.833	5	116.0	118.0
31.500	5	113.4	90.5
23.625	6	124.3	125.0
37.666	6	122.5	122.5
28.250	7	104.5	106.0
34.000	7	117.5	119.2
27.200	8	103.7	114.5
38.625	8	129.0	129.0
30.900	9	103.0	94.8
35.500	9	127.3	124.0
25.750	10	123.0	124.0
29.583	10	89.5	90.5
36.500	10	130.0	129.0

27

points. The spurious order, which is the sum of the harmonics of the undesired carrier plus the harmonics of the local oscillator, also is noted in Table III. The results for either injection mode basically meet or exceed the specification of interfering signals (i.e., removed at least ±500 kilohertz from the desired frequency), since performance is at least 80 dB above the 1.0-microvolt reference. The only response that did not meet the specification was the 53-megahertz image frequency for the circuit with the oscillator injected at gate 1; the signal was 77.5 dB above the reference.

The system performance of the AC coupled circuit of Figure 11 was evaluated in the same military FM receiver used for the direct-coupled circuit evaluations. Sensitivity, spurious response, cross-modulation distortion, and desensitization were measured at a frequency of 30 megahertz.

The results of sensitivity, desensitization, and spurious-response tests are listed in Tables IV, V, and VI, respectively. Sensitivity and desensitization data were similar to measurement data obtained with the direct-coupled configurations, although spurious response was somewhat poorer. The AC coupled RF amplifier-mixer circuit exceeded all contract specifications at 30 megahertz.

H. DESCRIPTION OF DESENSITIZATION MEASUREMENT

The desensitization measurement requires a large interfering signal to be injected into the front end, 1 megahertz removed from a threshold desired signal, at such a level that the audio output signal plus noise-to-noise ratio of 10 dB is reduced to 6 dB. This test has proven difficult to perform due to noise sidebands from the interfering signal generator entering the receiver. The dynamic range of the circuit under test was such that the noise from the generator and power amplifier could not be padded down and still be capable of supplying sufficient power to properly perform the measurement.

Therefore, an equivalent 2-dB-compression test was used in measuring desensitization. This alternate test consists of injecting an interfering signal, 1 megahertz removed from a small desired signal, at such a level as to reduce the output of the front end by 2 dB. The desired signal need only be small

28

TABLE IV. AUDIO OUTPUT (S+N)/N VERSUS RF SIGNAL
AT 30 MEGAHERTZ FOR AC COUPLED CIRCUIT

RF Signal (hard μV)	Audio Output (S+N)/N (dB)
1.05	26.0
1.00	25.0
0.60	19.0
0.50	16.0
0.40	12.5
0.35 *	10.0

*Front end sensitivity.

TABLE V. DESENSITIZATION AT 30 MEGAHERTZ
FOR AC COUPLED CIRCUIT

Interfering-Signal Frequency (MHz)	Signal Magnitude Above Reference Level of 0.35 μV (dB)
27.0	125.9
29.0	106.0
31.0	101.4
33.0	125.2

29

TABLE VI.   SPURIOUS RESPONSE AT 30 MEGAHERTZ
FOR AC COUPLED CIRCUIT

Spurious Frequency (MHz)	Spurious Order	Magnitude Above 1-μV Reference Level (dB)
53.000	2	80.1
15.000	3	97.0
26.500	3	90.6
17.666	4	115.1
35.750	4	97.1
23.833	5	113.2
31.500	5	90.4
23.625	6	119.9
37.666	6	115.4
28.250	7	102.6
34.000	7	109.3
27.200	8	106.2
38.625	8	122.6
30.900	9	89.6
35.500	9	117.7
25.750	10	119.0
29.583	10	87.0
36.500	10	123.8

compared to the interfering signal reaching the devices. It should not be a threshold signal which could be affected in level by noise. The dynamic range will be the ratio of the large interfering signal to the 10-dB (S+N)/N threshold signal and this number will be less than or equal to the number which would have been measured had it been possible to perform the required test. The justification of this statement follows:

The desensitization test calls for a reduction of the (S+N)/N ratio in the audio band from 10 dB to 6 dB. Using the equation,

$$\left(\frac{S}{N}\right)_{dB} = 10 \ \log \left[10^{\frac{1}{10}\left(\frac{S+N}{N}\right)_{dB}} - 1\right] \quad . \ . \ . \ . \ . \ . \ . \ . \ . \ . \ . \ . \ . \ . \ . \ (9)$$

the corresponding S/N ratios can be found to be 9.54 and 4.74 dB, respectively.

Using the FM detector curves of Figure 13[1] the carrier-to-noise ratio in the IF band, before the limiter, can be found from the ratios in the audio band. The necessary parameters are defined below.

IF Bandwidth B	= 34 kilohertz
Audio Bandwidth F	= 5.7 kilohertz
Frequency Deviation (f_d)	= ±8 kilohertz

$$\frac{B}{F} = \frac{34}{5.7} = 5.96 \quad . \ (10)$$

$$\frac{f_d}{F} = \frac{8.0}{5.7} = 1.41 \quad . \ . \ . \ . \ . \ . \ . \ . \ . \ . \ . \ . \ . \ . \ . \ . \ . \ . \ . \ (11)$$

$$20 \ \log_{10} \left(\frac{f_d}{F}\right) = 2.98 \ dB \ . \ . \ . \ . \ . \ . \ . \ . \ . \ . \ . \ . \ . \ . \ . \ . \ . \ (12)$$

The adjusted S/N ratios are 12.52 and 7.72 for the high and low points, respectively. From Figure 13 the corresponding carrier-to-noise ratios in the IF band, C/N, are found to be 7.4 dB and 5.4 dB.

---

[1] K. G. MacLean, Unpublished Report.
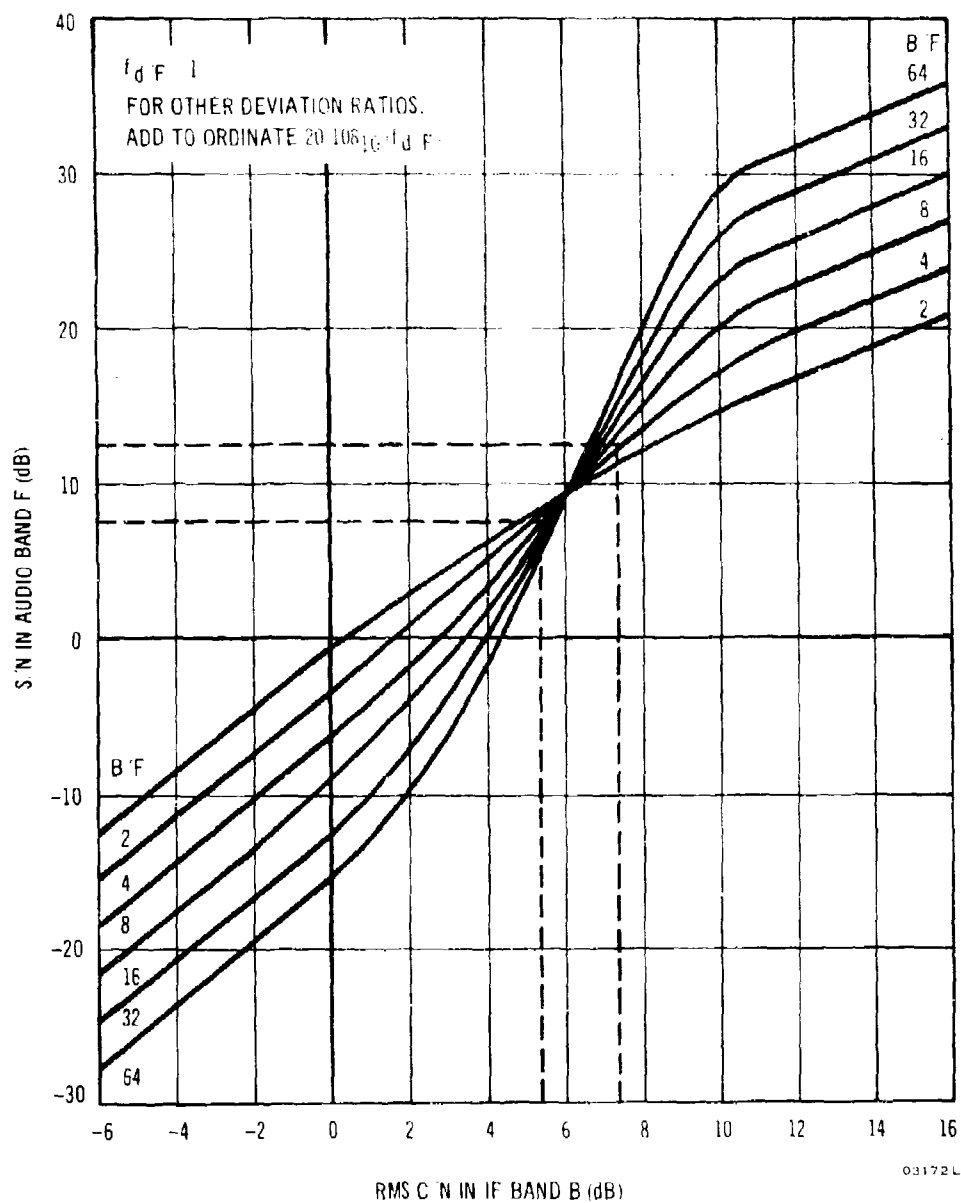
Figure 13. Signal-To-Noise Ratio in Audio Band vs. Carrier-To-Noise Ratio in IF Band

The signal-to-noise ratio at the output of the front end should be equal to the value in the IF band, if the gain of the front end is sufficient to make the noise contribution of the IF amplifier negligible. Correspondingly, the front end essentially is responsible for the degradation of the signal-to-noise ratio. There are two ways in which this can happen: the noise figure of the first RF stage can increase, and the gain of the first RF stage can decrease so that the noise figure of the second stage begins to add to the overall system noise figure. The cause of degradation actually will be combination of the two. Suziki and Toya[2] have shown that the gain will start to decrease before the noise figure increases. Therefore, the gain will fall 2 dB before the noise figure increases 2 dB. This signal deterioration occurs rapidly as the interfering-signal level increases beyond the dynamic range. It follows, therefore, that the decrease in C/N ratio from 7.4 dB to 5.4 dB will not occur before the gain has deteriorated by 2 dB.

I. DIRECT-COUPLED RF AMPLIFIER-MIXER CIRCUIT

The preliminary direct-coupled RF amplifier-mixer with the local oscillator injected at gate 1 and ground potential was modified to increase overall front-end gain and decrease quiescent power dissipation. The improved circuit, shown in Figure 14, contains only seven p-channel MOS enhancement devices. Transistors Q1 and Q2 are dual-gate devices for RF amplification and mixing, respectively. For this direct-coupled configuration, the mixer unit is biased, by a positive potential on gate 1 of transistor Q2, in the near optimum region for maximum gain and minimum quiescent power dissipation. The power gain of the mixer stage under neutralized matched-output conditions is given by

$$G_p = \frac{\left| g_{mc} \right|^2}{4 \mathrm{Re}(y_{11})_{RF} \, \mathrm{Re}(y_{22})_{IF}} \quad \ldots \ldots \ldots \ldots \ldots \ldots \ldots (13)$$

where

g_{mc} = conversion transconductance of the tetrode

$(y_{11})_{RF}$ = RF input admittance of the tetrode

$(y_{22})_{IF}$ = IF output admittance of the tetrode

[2] Suziki, Toya, "Desensitization in Transistorized PM Receivers," Electronics and Communications in Japan, 48, 48-95, January 1965.
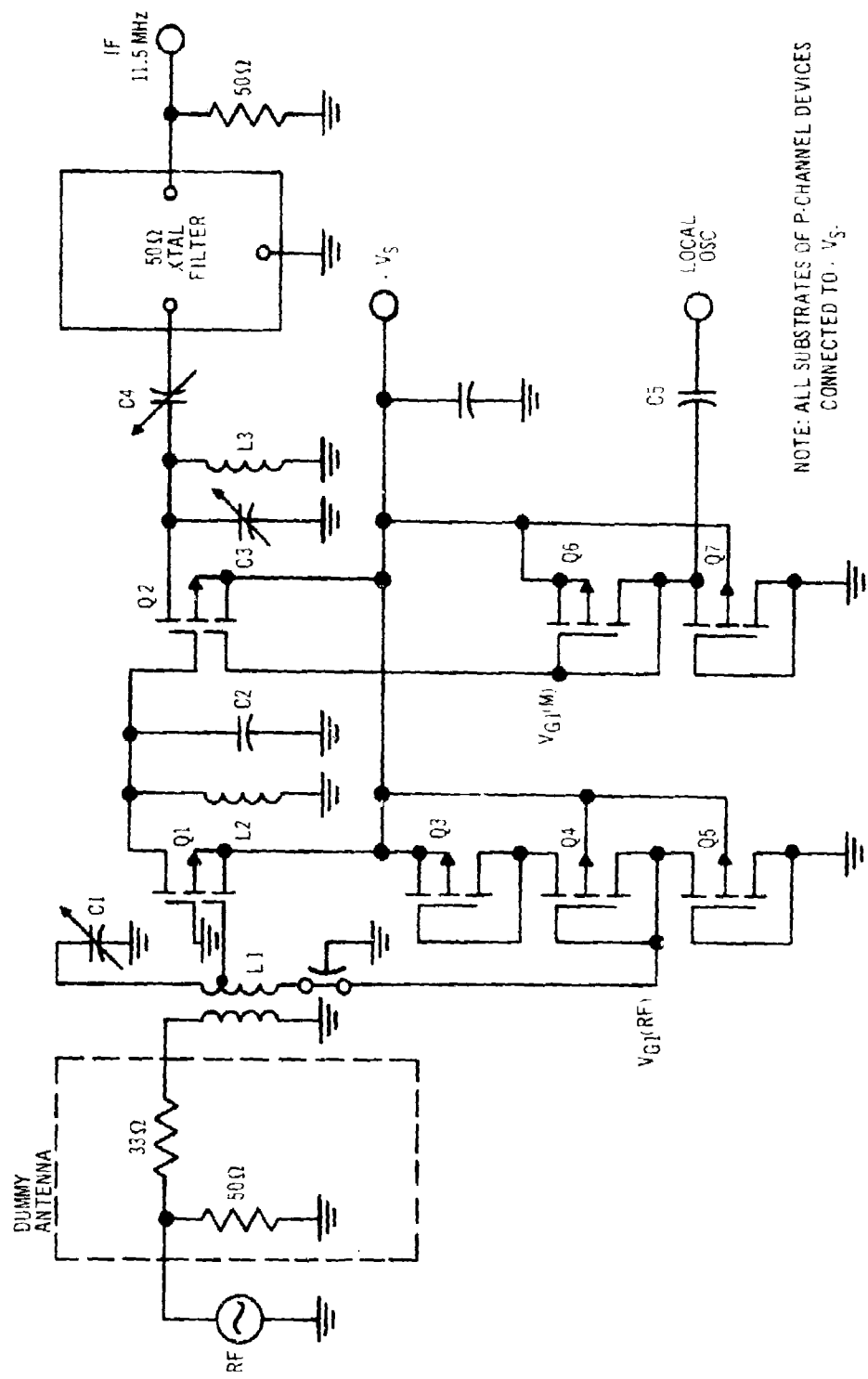
Figure 14. Direct-Coupled RF Amplifier-Mixer Circuit

NOTE: ALL SUBSTRATES OF P-CHANNEL DEVICES
CONNECTED TO V_S.

34

By reducing the source-to-gate 1 bias of transistor Q2, the conversion transconductance increases as shown in the curves of either Figure 5 or Figure 6. In addition, the input and output conductance of a tetrode unit, $Re(y_{11})$ and $Re(y_{22})$, respectively, decreases by lowering the source-to-gate 1 bias. It follows from Eq. (13), therefore, that the direct-coupled RF amplifier-mixer circuit of Figure 14 should exhibit a higher power gain than the preliminary direct-coupled circuit of Figure 9 with the local oscillator injected at ground potential.

The threshold-bias technique is incorporated to provide good DC stability of the RF amplifier stage. Conduction of MOS device Q5 is low, compared to units Q3 and Q4, so that the potential at gate 1 of transistor Q1, $V_{G1}(RF)$ is approximately $V_S - 2V_T$. Since the source-to-gate potential is essentially independent of supply voltage, the gain and quiescent drain current of the RF stage vary little with supply voltage. Devices Q6 and Q7 of Figure 14 are equal-geometry units that bias transistor Q2 at approximately one-half the supply voltage. These equal-size units allow the DC potential at gate 1 of device Q2, $V_{G1}(M)$ to be nearly independent of the magnitude of the local oscillator signal. When a threshold-bias scheme was substituted for devices Q6 and Q7, the DC voltage at gate 1 of unit Q2 depended significantly upon the magnitude of the local oscillator signal. Because of the nonlinear nature of MOS structures, large AC signals generally will upset the DC potential. Due to the symmetry associated with equal-geometry units Q6 and Q7, however, the nonlinear effects cancel, and DC bias is independent of large AC signals.

Inductor L1 and capacitor C1 provide selectivity and matching at the RF input; inductor L2 and capacitor C2 provide selectivity at the RF amplifier-mixer interstage. Inductor L3 and capacitors C3 and C4 provide selectivity and matching (to a 50-ohm crystal filter) at the mixer output. The 3-dB bandwidths at the crystal input are approximately 200 kilohertz at 30 megahertz and 500 kilohertz at 76 megahertz, while the 6-dB bandwidth at the crystal output is 32 kilohertz.

The circuit exhibited power gains of 35 dB at 30 megahertz and 34 dB at 76 megahertz with a 9-volt supply and a 3-volt-RMS local oscillator signal.

Power dissipation was approximately 120 milliwatts at 9 volts. The gain at 30 megahertz for a 3-volt-RMS oscillator magnitude varies little with supply, as shown in Table VII. Power dissipation was less than 90 milliwatts for an 8-volt supply. The direct-coupled RF amplifier-mixer circuit of Figure 14 exhibits an overall power gain that compares with the AC coupled circuit of Figure 11, while eliminating the need for an external interstage coupling capacitor and an additional pin in the IC package.

TABLE VII. POWER GAIN AT 30 MEGAHERTZ AND POWER
DISSIPATION VERSUS SUPPLY VOLTAGE FOR
DIRECT-COUPLED CIRCUIT

Supply Voltage (V)	Power Gain* (dB)	Power Dissipation (mW)
8.0	34.75	88.0
9.0	35.00	120.6
10.0	35.25	159.0

*Does not include the loss in the dummy antenna
and in the IF crystal filter.

J. SYSTEM PERFORMANCE OF DIRECT-COUPLED RF AMPLIFIER-MIXER CIRCUIT

The system performance of the direct-coupled RF amplifier-mixer circuit of Figure 14 was evaluated in the same test setup that was used for the previous front-end assemblies. Sensitivity, desensitization, and spurious response were measured at frequencies of 30 megahertz and 76 megahertz (41.5 and 64.5 megahertz local oscillator, respectively). All measurements were taken for a 9-volt supply and a 3-volt-RMS local oscillator. Table VIII shows the results of sensitivity tests at both 30 megahertz and 76 megahertz. The signal plus noise-to-noise ratio at 30 megahertz, which exceeded contract specifications, compared to the results of previous RF amplifier-mixer circuits. There was some improvement at 76 megahertz, however, where the sensitivity, including the loss in the dummy antenna, was 0.3 of a hard microvolt RF input signal with a 10 dB audio output (S+N)/N ratio.

TABLE VIII.   AUDIO OUTPUT (S+N)/N VERSUS RF SIGNAL INPUT AT 30
MEGAHERTZ AND 76 MEGAHERTZ FOR DIRECT-COUPLED CIRCUIT

RF Signal	Audio Output (S+N)/N (dB)	
(hard µV)	at 30 MHz	at 76 MHz
1.0	27.0	27.0
0.6		21.0
0.5		18.0
0.45	14.0	
0.40		13.0
0.35 *	10.0	12.0
0.30 *		10.0

*Sensitivity

The results of desensitization measurements at 30 megahertz and 76 mega-
hertz are shown in Tables IX and X, respectively. The results at 30 megahertz
exceed the desired specifications and show some improvement over the desensiti-
zation results for previous circuits (shown in Tables II and V). Spurious-
response data for the modified DC coupled circuit at 30 megahertz and 76 mega-
hertz are listed in Tables XI and XII, respectively. The results at 30 mega-
hertz indicate a considerable improvement over the spurious-response data for
previous circuits (shown for 30 megahertz in Tables III and VI). The modified
DC coupled circuit of Figure 14 not only exhibited higher gain with less
quiescent power dissipation than the DC coupled circuits of Figures 9 and 10,
but the desensitization and spurious-response performances at 30 megahertz
also were improved. Although spurious-response data at 76 megahertz were not
as good as the data at 30 megahertz, the circuit of Figure 14 met all contract
specifications except for image frequency (see spurious order 2 in Table XII).
Spurious response and desensitization can be improved, at some sacrifice in
gain and sensitivity, by lowering the tap on RF input coil L1. Since the gain
at 76 megahertz exceeds a practical front-end requirement, a design compromise
appears advantageous. Sensitivity, which was extremely good at 76 megahertz,
also can be compromised somewhat without any significant degradation in per-
formance.

TABLE IX. DESENSITIZATION RESULTS AT 30 MEGAHERTZ
FOR DIRECT-COUPLED CIRCUIT

Interfering-Signal Frequency (MHz)	Signal Magnitude Above 0.35-μV Reference Level (dB)
27.0	131.5
29.0	116.9
31.0	116.6
33.0	133.4

TABLE X. DESENSITIZATION RESULTS AT 76 MEGAHERTZ
FOR DIRECT-COUPLED CIRCUIT

Interfering-Signal Frequency (MHz)	Signal Magnitude Above 0.3-μV Reference Level (dB)
68.5	129.0
75.0	99.7
77.0	93.8
83.5	126.7

TABLE X1. SPURIOUS RESPONSE AT 30 MEGAHERTZ
FOR DIRECT-COUPLED CIRCUIT

Spurious Frequency (MHz)	Spurious Order	Magnitude Above 1-μV Reference Level (dB)
53.000	2	97.0
15.000	3	97.0
26.500	3	104.5
17.666	4	126.8
35.750	4	112.7
23.833	5	124.3
23.625	6	132.6
37.666	6	128.0
28.250	7	111.1
34.000	7	128.5
27.200	8	114.4
38.625	8	137.7
30.900	9	101.9
35.500	9	>140.0
25.750	10	129.6
29.583	10	107.5
36.500	10	>140.0
29.687	14	105.8
31.000	16	120.0
30.200	17	91.2
29.136	19	129.9
30.166	21	92.9
29.615	22	115.4
30.464	24	115.8
29.666	26	114.6
29.250	27	125.5
30.406	28	106.5

TABLE XII.   SPURIOUS RESPONSE AT 76 MEGAHERTZ
FOR DIRECT-COUPLED CIRCUIT

Spurious Frequency (MHz)	Spurious Order	Magnitude Above 1-µV Reference Level (dB)
53.000	2	64.2
38.000	3	88.8
117.500	3	80.0
58.750	4	108.5
70.250	4	84.6
46.833	5	123.6
91.000	5	108.4
60.666	6	122.0
68.333	6	104.3
51.250	7	127.5
82.166	7	97.0
67.375	8	112.3
103.666	8	124.5
53.900	9	129.9
77.750	9	85.8
83.500	9	104.2
66.800	10	118.5
93.875	10	126.7
75.100	11	89.6
75.357	15	84.6
76.250	22	101.6
75.181	24	100.0
76.208	26	94.9
75.307	28	100.4

K. TEMPERATURE EVALUATION OF RF AMPLIFIER-MIXER BREADBOARD CIRCUIT

The direct-coupled MOS RF amplifier-mixer breadboard circuit, shown in Figure 14, was evaluated for power gain and stability at 30 megahertz over the entire temperature range $-55^{\circ}C$ to $125^{\circ}C$. The values obtained for power gain at 30 megahertz, RF amplifier and mixer bias potentials, $V_{G1}(RF)$, and $V_{G1}(mixer)$ as a function of temperature are shown in Table XIII. Measurements were made with a local oscillator signal level of 3 volts RMS and with a supply level of 9 volts. Power gain was 35.0 dB at room temperature and increased slightly to 35.5 dB at $-55^{\circ}C$, demonstrating an essentially constant power gain at low temperatures. Power gain decreased at elevated temperatures, as expected; however, gain still was 28.0 dB at $75^{\circ}C$ and 20.0 dB at $125^{\circ}C$.

Table XIII indicates that the source-to-gate 1 bias of the RF amplifier transistor, which is approximately $2V_T$, decreased with increasing ambient temperature, as $V_{G1}(RF)$ increased. This decrease is caused by the drop in magnitude of the threshold voltage at elevated temperature. Note, however, that the source-to-gate 1 bias of the mixer dual-gate device, which is approximately equal to one-half the supply voltage, was essentially independent of temperature. Equal-geometry units Q6 and Q7, therefore, cause a gate 1 bias of transistor Q2 to be nearly independent of both local oscillator signal magnitude and temperature. The gain still may be adequate for some practical front-end designs (at least up to $100^{\circ}C$); in addition, the circuit was absolutely stable over the entire range of $-55^{\circ}C$ to $125^{\circ}C$.

An experiment was conducted to determine the loss in power gain caused by a decrease in threshold voltage (for increasing temperature). An external $V_{G1}(RF)$ bias of 5.2 volts was applied at $25^{\circ}C$, which exactly simulated the bias at $125^{\circ}C$. Under this condition, measured power gain was 34.5 dB, a change of only 0.5 dB from the normal 4.6-volt bias at room temperature. It appears, therefore, that the decrease in threshold voltage was not the primary cause of loss in gain at elevated temperature.

The temperature dependence of the surface mobility of electrons in silicon for n-channel structures has been reported by Fang and Triebwasser[3]. While

---

[3] F. Fang and S. Triebwasser, IBM Journal, _8_, 410 (1965).

TABLE XIII. POWER GAIN AT 30 MEGAHERTZ AND BIAS
POTENTIALS VERSUS TEMPERATURE FOR DIRECT-COUPLED CIRCUIT

Temperature (^{o}C)	Power Gain (dB)	V_{G1}(RF) (V)	V_{G1}(M) (V)
-55	35.5	4.40	4.75
-25	35.5	4.40	4.75
0	35.5	4.50	4.75
25	35.0	4.60	4.80
50	33.0	4.65	4.75
75	28.0	4.75	4.75
100	24.0	4.90	4.75
125	20.0	5.20	4.75

surface mobility is highly dependent upon surface treatment and oxidation conditions, it was found that a decrease in mobility can be expected with increasing temperature. The results are similar for the surface mobility of holes in silicon, which would be the case for p-channel devices. Therefore, it can be concluded that some of the loss in power gain was caused by the decrease in mobility (at elevated temperature). In addition, no special effort was made to use passive components, i.e., resistors, capacitors, and inductors, which minimized variations in characteristics over the specified temperature range. It is therefore possible that the passive elements could have also contributed to the loss in gain over temperature.

L. VARACTOR-TUNING OF DIRECT-COUPLED RF AMPLIFIER-MIXER BREADBOARD CIRCUIT

One objective of this program was to investigate voltage-variable capacitors (varactors) for tuning the MOS RF amplifier-mixer circuit. Although a single set of varactors, used at the RF input and at the RF amplifier-mixer interstage, could be made to tune over the entire range of 30 to 76 megahertz, this scheme would degrade cross-modulation and desensitization performance. The system approach was to divide the 30-to-76-megahertz receiver into four separate frequency bands. The direct-coupled RF amplifier-mixer circuit of Figure 14 was modified to incorporate varactor tuning. The circuit shown in Figure 15 was designed, breadboarded, and tested over the 53-to 63-megahertz band.

The breadboard circuit incorporated a matched pair of TRW varactors (part number PG3247BT2D), 47 picofarads ±5 percent, at a reverse bias, V_R, of 4 volts and a quality factor, Q, of 300 at V_R = 4 volts and a frequency of 50 megahertz. Individual units exhibited a minimum capacitance ratio of 3:1 at reverse-bias levels of 4 volts and 50 volts and tracked to within a maximum of 1 percent of each other from V_R = 0.5 volt to 50 volts. The minimum reverse breakdown voltage was 50 volts, with a maximum leakage current of 500 nanoamperes (at 50 volts).

It is desirable to use a single control voltage for tuning the front end. The required RF input and RF output bias voltages are incompatible with the tuning voltage for the voltage-variable capacitors. Therefore, capacitors C6 and C7 are used to AC couple varactors CR1 and CR2 to the RF input and the
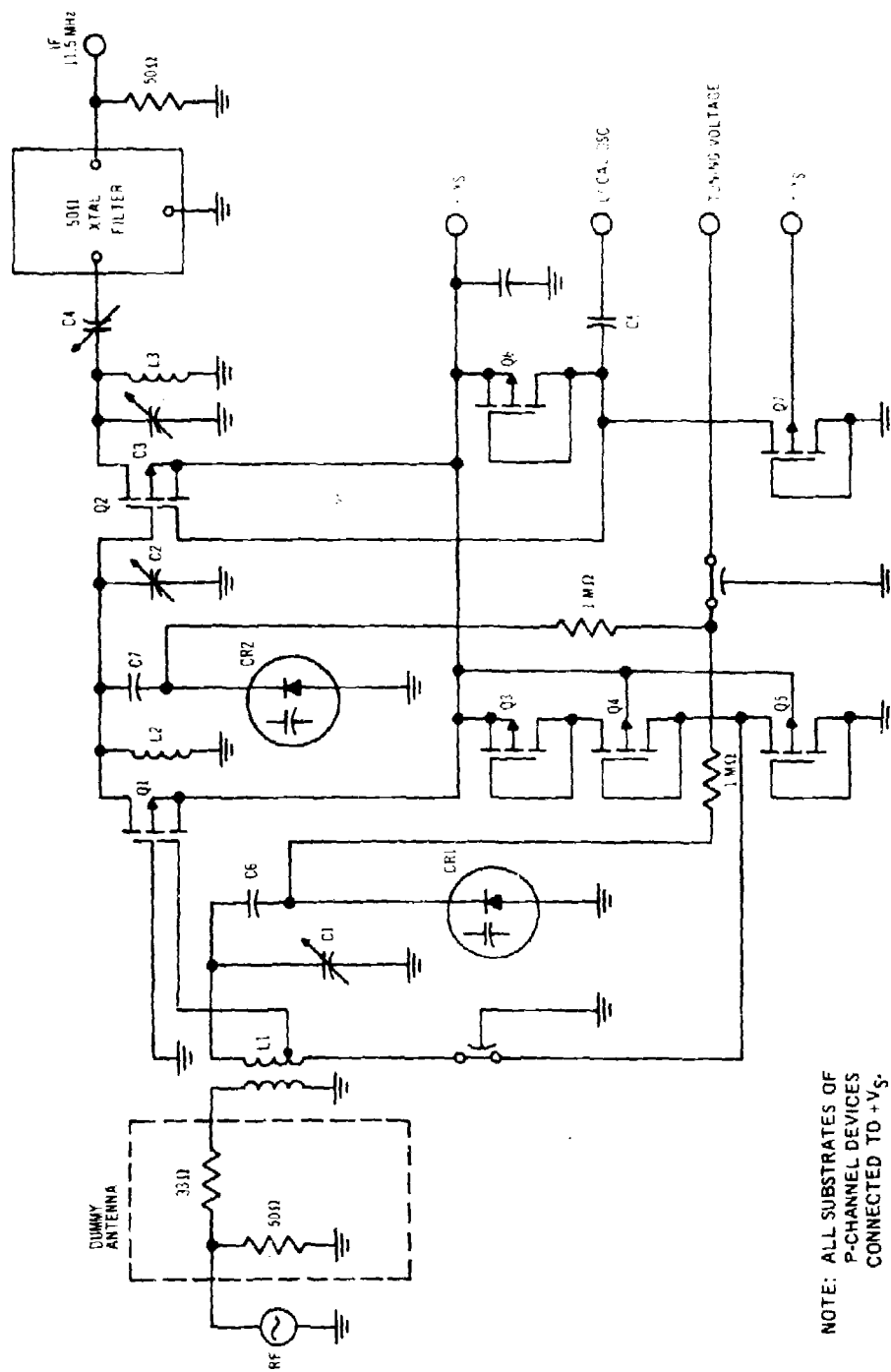
Figure 15. Varactor-Tuned RF Amplifier-Mixed Circuit

NOTE: ALL SUBSTRATES OF
P-CHANNEL DEVICES
CONNECTED TO +V$_S$.

44

amplifier-mixer interstage, respectively. Capacitors Cl and C2 are necessary
to minimize tracking errors by compensating the effects of stray circuit capaci-
tance and the difference between diode characteristics. The 1-megohm resistors
are inserted to prevent loading due to the tuning control circuit.

Variations in power gain as a function of frequency over the 53-to 63-mega-
hertz band are plotted in Figure 16. Measurements were taken for a 3-volt-RMS
local oscillator signal and a 9-volt supply. The gain, which was 29.0 dB and
31.5 dB at 53 and 63 megahertz, respectively, varied 2.5 dB over the frequency
range. Figure 17 shows the single tuning voltage required as a function of
frequency. The front end was tuned at 53 and 63 megahertz with 10 and 31
volts, respectively. A control voltage of 17.5 volts tuned the assembly at
58 megahertz, which is midband, at which power gain was 30.5 dB. The varactor
loading at the RF amplifier-mixer interstage was mainly responsible for the
loss in power gain over the frequency band.

M. FABRICATION OF INTEGRATED MOS RF AMPLIFIER-MIXER CIRCUIT

Based on the results obtained during the investigation of the breadboard
portion of the program, it was decided to build the direct-coupled circuit of
Figure 14 in integrated-circuit form. The IC consists of two 0.2-mil channel
length dual-gate transistors for the RF amplifier and mixer stages, and fiv·
0.3-mil channel length triodes that are used for internal biasing. The seven
p-channel, MOS devices, fabricated on a common substrate, are noted in the
schematic of Figure 18. Only the two dual-gate transistors were required to
be designed with high-frequency technology that minimizes feedback capacitance.
After completing the photomasks, the following steps were taken in successfully
processing the integrated circuit:

  a. Initial Cleaning and Oxidation - A 10-ohm-cm n-type wafer is
      used. Initially, the wafer received for processing is 6-mils
      thick and has one chemically polished face which is used for the
      device. The back is lapped. The first step in processing is a
      careful cleaning of the wafer to remove all contamination. Then
      an oxide layer is thermally grown to a thickness of about 2000Å
      to provide a diffusion mask.
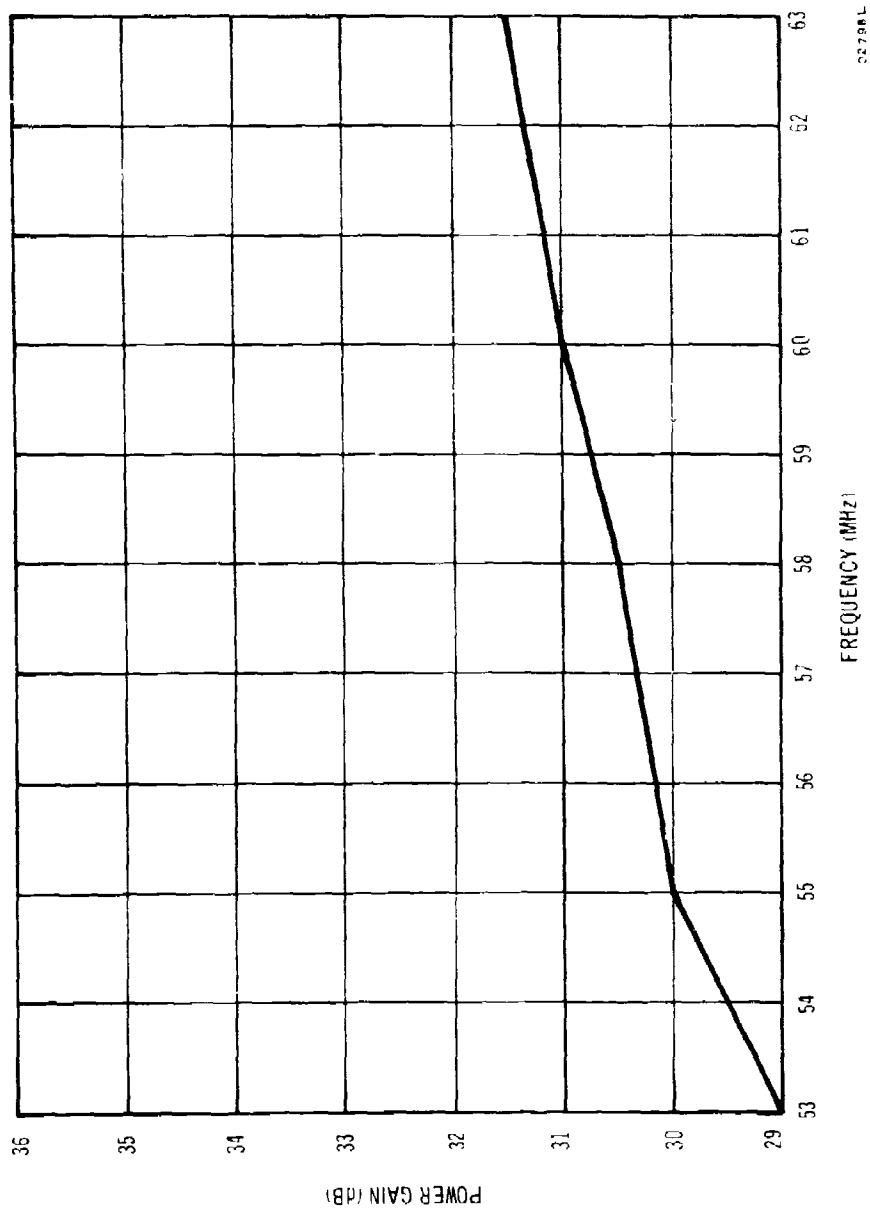
Figure 16. Power Gain vs. Frequency, 53 to 63 Megahertz

46
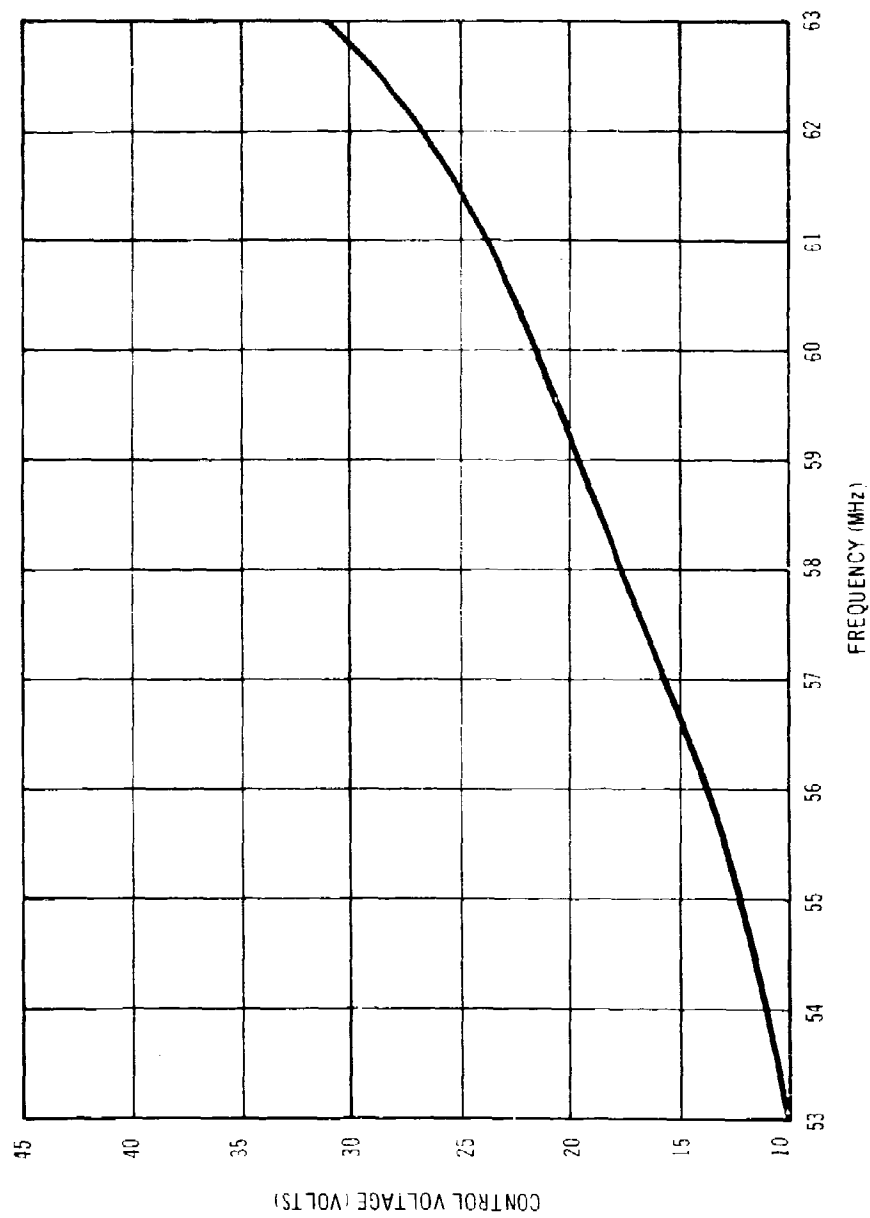
Figure 17. Control Voltage vs. Frequency, 53 to 63 Megahertz

027 96 L

47
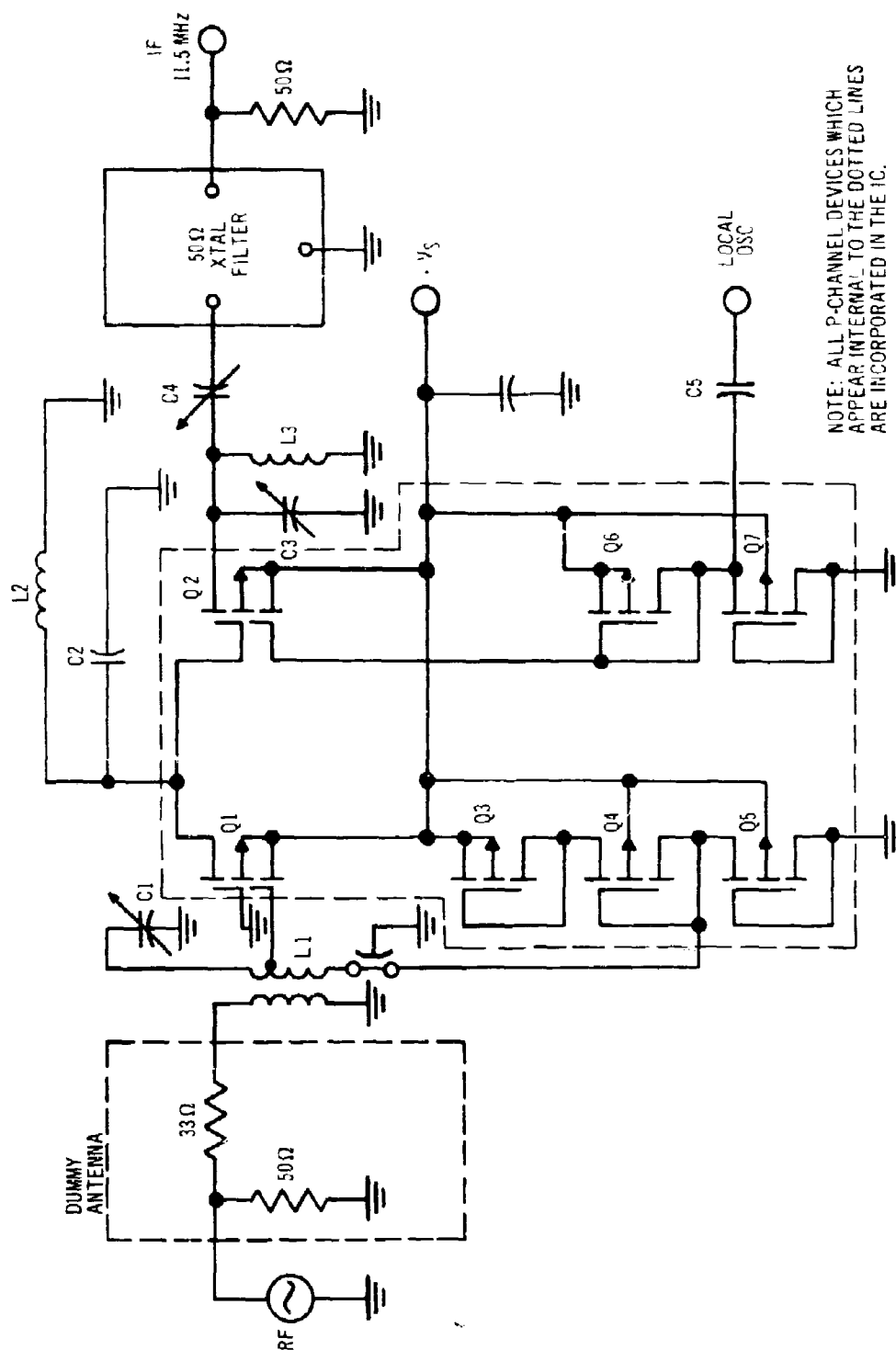
Figure 18. Schematic of Integrated MOS RF Amplifier-Mixer Circuit

NOTE: ALL P-CHANNEL DEVICES WHICH APPEAR INTERNAL TO THE DOTTED LINES ARE INCORPORATED IN THE IC.

48

b. **Source and Drain Diffusion** - The source and drain areas are
    opened in the oxide by using standard photolithographic and
    oxide-etching techniques. The openings for the source and drain
    regions of the dual-gate structures are of intermediate size -
    smaller than the actual source and drain of the finished tran-
    sistor, but larger than the source-drain contact areas. The
    openings for the bias triodes are close to the actual size re-
    quired for the source-drain areas. A boron nitride source at
    1100°C in an oxygen-nitrogen atmosphere is used for diffusion.
    The resultant surface concentration of boron is greater than
    10^{19}/cc and the junction depth is about 0.04 mil.

c. **Strip Boron Glass** - The masking oxide becomes covered with a
    boron-based glass layer during the source-drain diffusion. A
    10-percent hydrofluoric-acid etch followed by a hot-nitric-acid
    soak is used to remove this layer.

d. **Define Active Areas** - About $2000\overset{\circ}{A}$ of oxide are deposited on the
    wafer. The active regions of the transistor are defined and the
    oxides in these regions are removed by standard photolithographic
    and etching techniques.

e. **Definition of Channel and Contact Regions** - One of the features
    of the high-frequency dual-gate structure is the thick oxide step
    at the edge of the channel. This step is fabricated by deposit-
    ing a thick layer of oxide (from 5000 to $8000\overset{\circ}{A}$) over the entire
    wafer. The channel regions are defined; then the oxide in the
    channel is removed by etching. An oxide step, located at the
    edge of the channel, remains. During this procedure the thick
    deposited oxide is removed over the active regions of the triodes
    as well as from all contact regions. At this stage the deposited
    oxide etches rapidly. After high-temperature densification in
    succeeding steps, the time required for the etch to go through
    the thick oxide layers to open contacts would be prohibitive.

f. **Channel Oxide** - The next step is the formation of the channel
    oxide by a combination of thermal oxidation and deposited oxide.

49

High-temperature densification follows. An initial thermal oxide of about 400Å passivates the silicon surface in the channel region. A phosphorus-doped oxide is then deposited to insure stability of the channel oxide. The total channel oxide is 600 to 800Å.

g. <u>Channel Anneal</u> – After channel oxidation, the amount of fixed oxide charge at the silicon-oxide interface is minimized by annealing in hydrogen for 15 minutes at 450°C. This step is crucial in our process for obtaining low threshold (1 to 2 volts) on p-channel transistors.

h. <u>Final Opening of Ohmic Contact Areas</u> – The channel oxide of the previous step also forms over the contact regions that had been opened previously. This oxide is removed from the contact areas by standard photolithographic and etching techniques.

i. <u>Metalization</u> – Aluminum metalization, evaporated on the room temperature substrate, is used for all electrodes. The aluminum is defined by photolithographic processes and is etched with phosphoric acid. The final photoresist is removed in hot J-100, a commercial photoresist solvent.

j. <u>Bonding and Sealing</u> – The wafer is scribed in the standard manner used in IC manufacturing and the pellets then are mounted to the headers. Bonding is done on standard ultrasonic bonders using 1-mil aluminum wire. The transistors are baked in dry nitrogen and sealed in dry empty shells in a nitrogen atmosphere. The package used is a standard 10-lead TO-5. A photomicrograph of the 30- by 40-mil RF amplifier-mixer IC pellet appears in Figure 19.

N. <u>EVALUATION OF INTEGRATED MOS RF AMPLIFIER-MIXER CIRCUIT</u>

The integrated MOS RF amplifier-mixer circuit was evaluated in the same military FM receiver as that used for the front-end breadboard assemblies. Gain, sensitivity, desensitization, and spurious response were measured at frequencies of 30 and 76 megahertz.

INTERSTATE TUNING (5)

GATE 2 BIAS (6)

IF OUTPUT (3)

RF INPUT (7)

EXTRA POSITIVE SUPPLY (2)

GATE 1 BIAS (8)

LOCAL OSCILLATOR (1)

POSITIVE SUPPLY (10)

GROUND (9)
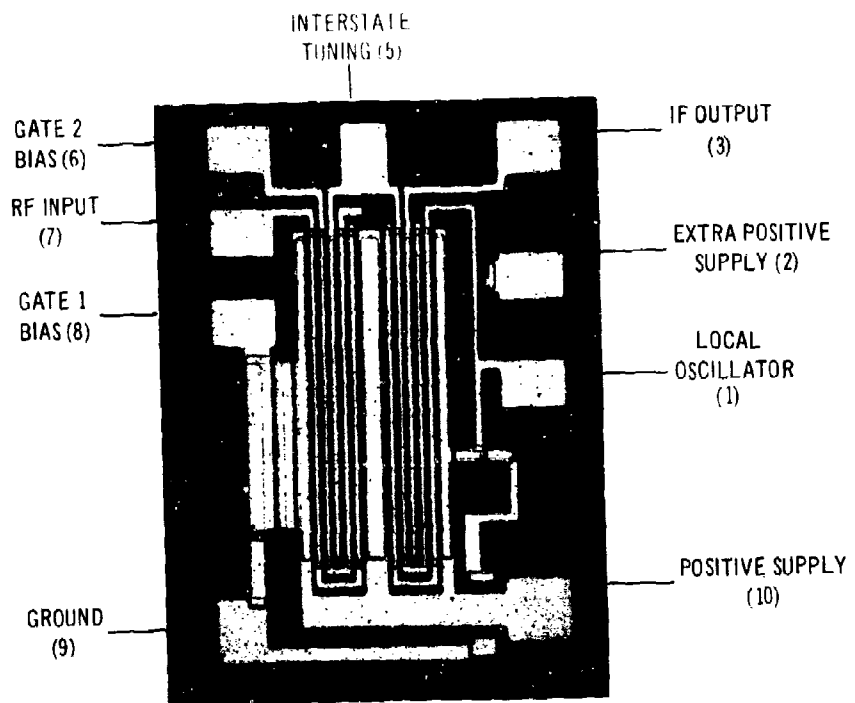
NOTE: PIN 4 – OPEN   03405P

Figure 19. Photomicrograph of the RF Amplifier-Mixer IC Pellet

51

Power gain at both 30 and 76 megahertz, and power dissipation, as a function of supply voltage are shown in Table XIV for a 3-volt-RMS local oscillator signal. The circuit exhibited a power gain of 34.0 dB at both 30 and 76 megahertz, with a typical power dissipation of 103.5 milliwatts, for a 9-volt supply. The power gain was 33.5 dB and 32.0 dB at 30 and 76 megahertz, respectively, with a reduced power dissipation of 52.5 milliwatts, for a 7-volt supply. The integrated circuit exhibited low power dissipation, 20.0 milliwatts, for a 5-volt supply where the power gain was 30.5 dB and 28.0 dB at 76 megahertz, respectively.

The power gain of the RF amplifier and mixer stage at 30 megahertz was 11.0 dB and 23.0 dB, respectively, for a 9-volt supply. At 76 megahertz the power gain of the RF amplifier and mixer stage was 14.0 dB and 20.0 dB, respectively, for a 9-volt supply. The power gain of the RF stage increased with frequency, while the mixer gain decreased with frequency. From Eq. (1) it can be demonstrated that under matched-input conditions, the power gain of the RF stage would decrease with frequency also (as does the mixer). But due to circuit instability, it was necessary to mismatch the input at 30 megahertz, with some sacrifice in RF power gain. However, the circuit was quite stable under matched input termination at 76 megahertz. Due to mismatching the input over the lower frequency band, therefore, the power gain of the RF stage actually increased with frequency. The power gain of each stage at 76 megahertz coincides closely with the values calculated from measured device parameters. The gain of the RF amplifier stage is given by

$$G_p = \frac{\left| y_{21} \right|^2 \operatorname{Re} y_L}{\left| y_{22} + y_L \right|^2 \operatorname{Re} y_{11}} \quad \ldots \ldots \ldots \ldots \ldots \ldots (14)$$

where y_L is the output load admittance of the RF stage, equal to the input at the second gate of the mixer stage, and it has been assumed that $y_{12} \approx 0$. The reactive components of y_{22} and y_L have been tuned out at the RF amplifier-mixer interstage, so that Eq. (14) reduces to

$$G_p = \frac{\left| y_{21} \right|^2 \operatorname{Re} y_L}{\left| \operatorname{Re} y_{22} + \operatorname{Re} y_L \right|^2 \operatorname{Re} y_{11}} \quad \ldots \ldots \ldots \ldots \ldots \ldots (15)$$

TABLE XIV. POWER GAIN AND DISSIPATION AT 30 MEGAHERTZ
AND 76 MEGAHERTZ VERSUS SUPPLY VOLTAGE FOR IC

Supply Voltage (V)	Power Gain (dB)*		Power Dissipation (mW)
	(30 MHz)	(76 MHz)	
5.0	30.5	28.0	20.0
6.0	32.5	30.5	36.0
7.0	33.5	32.0	52.5
8.0	34.0	33.0	76.0
9.0	34.0	34.0	103.5
10.0	34.5	34.5	130.0

*Does not include the loss in the dummy
antenna and in the IF crystal filter.

The parameters of transistor Q1 of Figure 18 are typically

$$|y_{21}| = 3.6 \times 10^{-3} \quad \ldots \ldots \ldots \ldots \ldots \ldots \ldots (16)$$

$$Re(y_{11}) = \frac{1}{6} \times 10^{-3} \quad \ldots \ldots \ldots \ldots \ldots \ldots \ldots (17)$$

$$Re(y_{22}) = \frac{1}{5} \times 10^{-3} \quad \ldots \ldots \ldots \ldots \ldots \ldots \ldots (18)$$

and $\quad Re(y_L) = \frac{1}{65} \times 10^{-3} \quad \ldots \ldots \ldots \ldots \ldots \ldots \ldots (19)$

Substituting these parameters into Eq. (15), the power gain of the RF amplifier in dB is given by

$$G_p = 10 \log_{10} \frac{(3.6 \times 10^{-3})^2 \frac{1}{65} \times 10^{-3}}{\left|\frac{1}{5} \times 10^{-3} + \frac{1}{65} \times 10^{-3}\right|^2 \times \frac{1}{6} \times 10^{-3}} \quad \ldots \ldots (20)$$

which is equal to

$$G_p = 14.1 \text{ dB} \ldots \ldots \ldots \ldots \ldots \ldots \ldots \ldots \ldots \ldots (21)$$

The power gain of the mixer stage is given by Eq. (13), where the parameters of transistor Q2 of Figure 18 are typically

$$|g_{mc}| = 1.0 \times 10^{-3} \quad \ldots \ldots \ldots \ldots \ldots \ldots \ldots (22)$$

$$Re(y_{11}) \text{ RF} = \frac{1}{65} \times 10^{-3} \quad \ldots \ldots \ldots \ldots \ldots \ldots (23)$$

and $\quad Re(y_{22}) \text{ IF} = \frac{1}{10} \times 10^{-3} \quad \ldots \ldots \ldots \ldots \ldots (24)$

Upon substitution of the above parameters into Eq. (13), the power gain of the mixer stage in dB is given by

$$G_p = 10 \log_{10} \frac{\left|1 \times 10^{-3}\right|^2}{4 \times \frac{1}{65} \times 10^{-3} \times \frac{1}{10} \times 10^{-3}} \quad \ldots \ldots \ldots (25)$$

which reduces to

$$G_p = 22.1 \text{ dB} \ldots \ldots \ldots \ldots \ldots \ldots \ldots \ldots \ldots \ldots (26)$$

The total gain is obtained by adding the amplifier and mixer gains (in dB) which results in 36.2 dB. Consequently, the results of Eq. (21) and (26) indicate that the calculated and measured power gain of each stage are in agreement.

The power gain of the RF amplifier-mixer IC was measured at 30 megahertz as a function of temperature, for a local oscillator signal level of 3 volts RMS and a 9-volt supply. Power gain was 34.0 dB at room temperature and increased slightly to 36.5 dB at -55°C. As expected from previous breadboard results, the power gain decreased at elevated temperatures. The measured power gain was 30.0 dB and 25.0 dB at 75°C and 125°C, respectively, which is adequate for most practical front-end designs. In addition, the integrated circuit was absolutely stable over the entire temperature range of -55°C to 125°C.

The results of the sensitivity tests for the IC at both 30 and 76 megahertz are given in Table XV. The sensitivity, including the loss in the dummy antenna, was 0.35 and 0.4 of a hard microvolt RF input signal for a 10-dB audio output (S+N)/N ratio, at 30 and 76 megahertz, respectively. Similar to previous breadboard results, these values exceeded contract specifications.

The results of desensitization measurements at 30 and 76 megahertz are shown in Tables XVI and XVII, respectively. The values obtained at 30 megahertz are similar to the breadboard results given in Table IX, while the results of the IC at 76 megahertz are not quite as good as those noted in Table X. Nevertheless, the contract specifications were easily exceeded in all cases. Spurious-response data for the integrated circuit at 30 and 76 megahertz are listed in Tables XVIII and XIX, respectively. Although the spurious-response performance at 30 megahertz was generally not as good as the breadboard results of Table XI, the contract requirements were exceeded in all cases. Except for the image frequency of 53 megahertz and a spurious frequency of 117.5 megahertz, the circuit met all specifications at 76 megahertz. All system measurements concerning sensitivity, desensitization, and spurious response were taken for a 9-volt supply and a 3-volt-RMS local oscillator signal.

TABLE XV. AUDIO OUTPUT (S+N)/N VERSUS RF SIGNAL INPUT
AT 30 MEGAHERTZ AND 76 MEGAHERTZ FOR IC

RF Signal	Audio Output (S+N)/N (dB)	
(Hard μV)	(30 MHz)	(76 MHz)
1.0	25.5	23.0
0.6		16.5
0.4*	11.0	10.0
0.35*	10.0	

*Sensitivity

TABLE XVI. IC DESENSITIZATION RESULTS AT 30 MEGAHERTZ

Interfering-Signal Frequency (MHz)	Signal Magnitude Above 0.35-μV Reference Level (dB)
27.0	128.0
29.0	117.4
31.0	116.3
33.0	133.2

TABLE XVII. IC DESENSITIZATION RESULTS AT 76 MEGAHERTZ

Interfering-Signal Frequency (MHz)	Signal Magnitude Above 0.4-μV Reference Level (dB)
68.5	124.2
75.0	97.0
77.0	90.0
83.8	121.8

TABLE XVIII. IC SPURIOUS RESPONSE AT 30 MEGAHERTZ

Spurious Frequency (MHz)	Spurious Order	Magnitude Above 1-μV Reference Level (dB)
53.000	2	99.3
15.000	3	87.6
26.500	3	96.4
17.666	4	125.6
35.750	4	102.4
23.833	5	117.4
23.625	6	122.9
37.666	6	122.3
28.250	7	112.3
34.000	7	122.3
27.200	8	109.5
38.625	8	120.8
30.900	9	98.1
35.500	9	124.6
25.750	10	123.5
29.583	10	88.9
36.500	10	122.6
29.687	14	87.2
31.000	16	103.2
30.200	17	76.6
29.136	19	115.1
30.166	21	79.7
29.615	22	94.6
30.464	24	88.6
29.666	26	101.9
29.250	27	115.3
30.406	28	90.1

TABLE XIX.   IC SPURIOUS RESPONSE AT 76 MEGAHERTZ

Spurious Frequency (MHz)	Spurious Order	Magnitude Above 1-μV Reference Level (dB)
53.000	2	63.5
38.000	3	86.6
117.500	3	76.3
58.750	4	105.6
70.250	4	84.1
46.833	5	117.1
91.000	5	108.0
60.666	6	119.7
68.333	6	106.2
51.250	7	124.6
82.166	7	101.6
67.375	8	113.3
103.666	8	122.8
53.900	9	124.5
77.750	9	85.3
83.500	9	108.8
66.800	10	117.1
93.875	10	124.3
75.100	11	85.8
75.357	15	82.9
76.250	22	88.3
75.181	24	90.1
76.208	26	85.3
75.307	28	89.1

O. <u>EVALUATION OF VARACTOR-TUNED RF AMPLIFIER-MIXER IC ASSEMBLY</u>

The MOS RF amplifier-mixer IC was incorporated into a varactor-tuned assembly and evaluated over the 63- to 76-megahertz band. A detailed schematic of the assembly appears in Figure 20, where the devices integrated are noted. An accompanying pin diagram of the TO-5 package is shown in Figure 21. The assembly uses a matched pair of Sylvania varactors (type D6909), with a higher Q than the TRW components associated with the circuit breadboard. The D6909 varactor diodes exhibited a nominal capacitance of 22 picofarads, at a reverse bias of 4 volts and a frequency of 1 megahertz, with a typical capacitance ratio of 3:1 at reverse-bias levels of 2 and 30 volts. The varactor Q was a minimum of 500 at $V_R = 4$ volts and a frequency of 50 megahertz. The minimum reverse breakdown was 30 volts, with a maximum leakage current of 10 micro-amperes (at 30 volts).

Variations in power gain and sensitivity as a function of frequency over the 63- to 76-megahertz band are listed in Table XX. The measurements were made for a 9-volt power supply and a 3-volt-RMS local oscillator level. The gain, which was 31.0 dB and 32.5 dB at 63 and 76 megahertz, respectively, varied 2.5 dB over the frequency range. The power gain was 33.5 dB at a frequency of 66 megahertz. The sensitivity varied from 0.4 to 0.5 of a hard microvolt RF input signal at 70 and 63 megahertz, respectively. The sensitivity, which averaged 0.45 microvolt, was slightly higher than usual due to the loss in the dummy antenna exceeding the normal 6 dB over the frequency band. Figure 22 shows the tuning voltage required as a function of frequency. The front end was tuned at 63 and 76 megahertz with 5.0 and 30.5 volts, respectively. A control voltage of 12.6 volts tuned the assembly at 70 megahertz, which is close to midband.

The results of desensitization measurements for the varactor-tuned assembly at 63, 70, and 76 megahertz, appear in Tables XXI, XXII, and XXIII, respectively. The performance was very good, with the contract specifications easily exceeded over the entire band. Spurious-response data at 76 megahertz are shown in Table XXIV. Again, except for the two spurious frequencies at 53 and 117.5 megahertz, the varactor-tuned front-end IC met the contract requirements. In addition, as specified, no permanent damage resulted to the RF amplifier-mixer IC assembly from the application of a 10-volt-RMS RF input signal level.

59

CR2

L1

CONTROL
VOLTAGE

1 MEG

0.01 µF

C4

C3

1 MEG

L2

C5

5

IF OUT TO
CRYSTAL FILTER
11.5 MHz

6

3

7

10, 2

+V_S = 9 V

0.01 µF

C2

33 Ω

50 Ω

C1

RF
INPUT

CR1

0.01 µF

50 Ω

LOCAL
OSCILLATOR

8

IC UNIT

0.01 µF

9
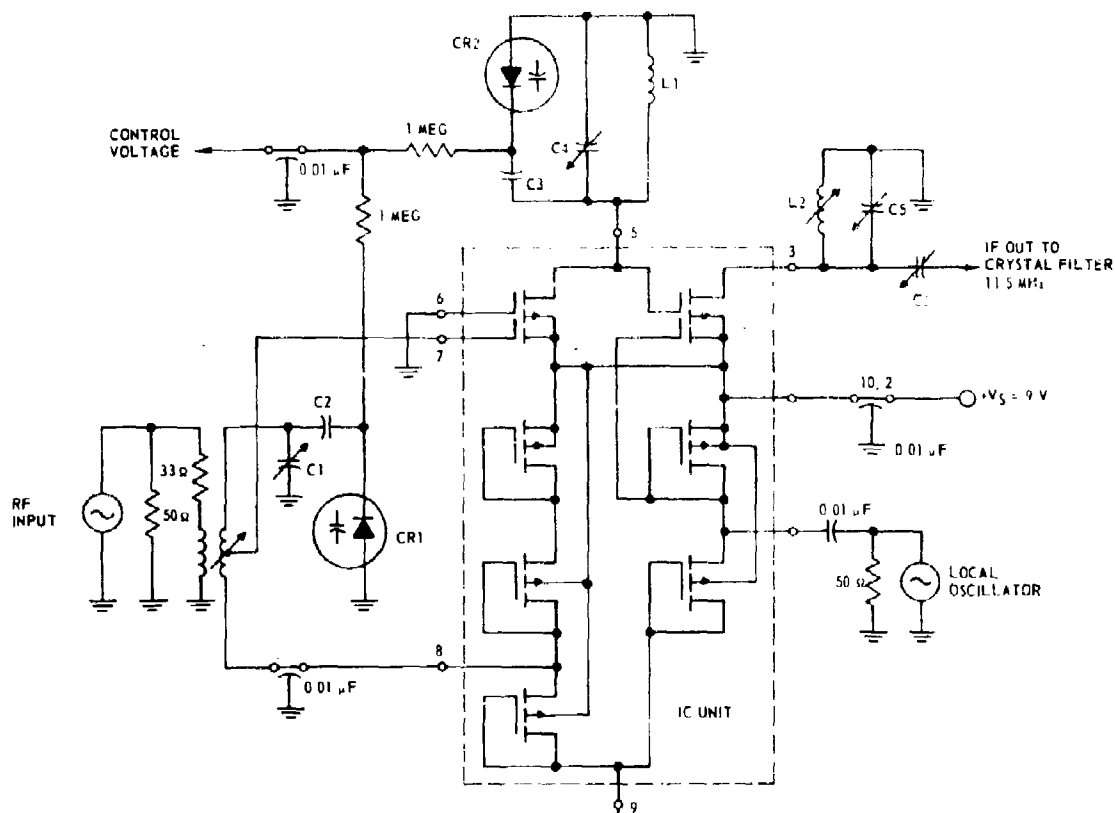
TRANSFORMER: PRIMARY = 2-3 T NO. 24 FORMVAR
SECONDARY = 8 T NO. 24 FORMVAR, TAP AT 5 T, L≈0.25 µH
CAMBION COIL FORM NO. 1536-7, BLUE SLUG (ADJUSTED SEVERAL TURNS IN TO TRIM INPUT
IMPEDANCE OVER THE 63-TO 76-MHz BAND)

C1 = 2 TO 8 pF   L1≈0.23 µH AIR COIL (5 T NO. 20, D = 3.8", L = ½")
C2 = 51 pF   L2≈2.4 µH (J.W. MILLER NO. 40 A 336CBI)
C3 = 750 pF   D1, D2 = SYLVANIA VOLTAGE-VARIABLE CAPACITOR DIODES,
C4 = 7 TO 25 pF   TYPE D6909 MATCHED PAIR; Q ≈ 500, RATIO
C5, C6 = 15 TO 60 pF C_{2V}/C_{30V} = 3, C_{a2V} ≈ 28.5 pF, C_{a30V} ≈ 9.5 pF
                              (DATA OBTAINED FROM MFG DATA SHEET)

NOTE: SUBSTRATE OF ALL P-CHANNEL DEVICES CONNECTED TO 9-VOLT SUPPLY

03174L

Figure 20. Schematic of Varactor-Tuned RF Amplifier-Mixer IC Assembly

60

BOTTOM VIEW

03175L
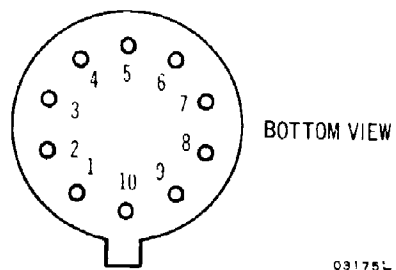
Figure 21. Pin Diagram of TO-5 IC Package
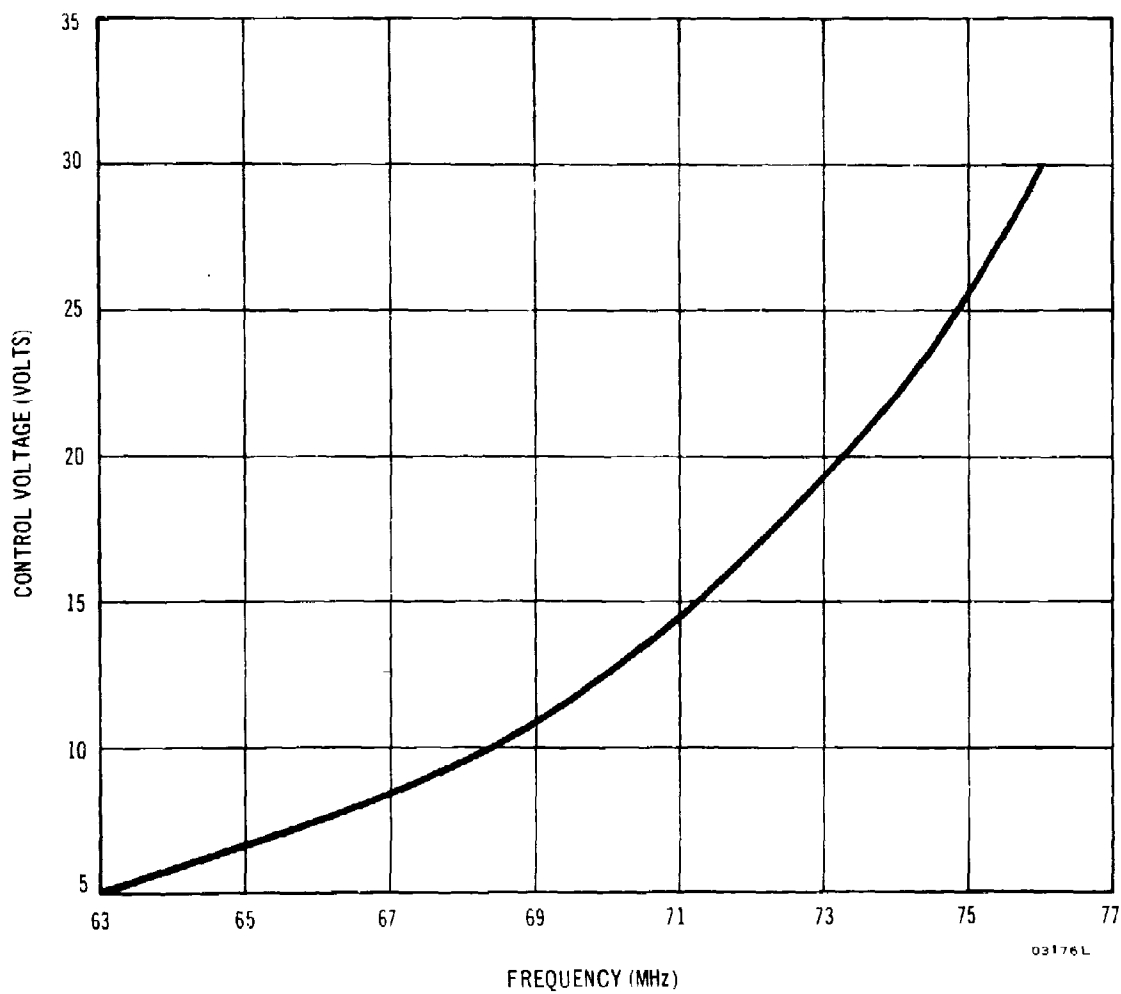
Figure 22. Control Voltage vs. Frequency for IC Over 63-To 76-Megahertz Band

TABLE XX. POWER GAIN AND SENSITIVITY VERSUS FREQUENCY
FOR VARACTOR-TUNED IC ASSEMBLY

Frequency (MHz)	Power Gain (dB)	Sensitivity (Hard µV)
63	31.0	0.50
66	33.5	0.45
70	32.5	0.40
73	32.0	0.45
76	32.5	0.45

TABLE XXI. DESENSITIZATION RESULTS FOR VARACTOR-
TUNED IC ASSEMBLY AT 63 MEGAHERTZ

Interfering-Signal Frequency (MHz)	Signal Magnitude Above Reference Level (dB)
56.7	126.8
62.0	101.4
64.0	95.8
69.3	123.4

63

TABLE XXII. DESENSITIZATION RESULTS FOR VARACTOR-
TUNED IC ASSEMBLY AT 70 MEGAHERTZ

Interfering-Signal Frequency (MHz)	Signal Magnitude Above Reference Level (dB)
63.0	126.9
69.0	119.6
71.0	116.6
77.0	126.2

TABLE XXIII. DESENSITIZATION RESULTS FOR VARACTOR-
TUNED IC ASSEMBLY AT 76 MEGAHERTZ

Interfering-Signal Frequency (MHz)	Signal Magnitude Above Reference Level (dB)
68.4	125.0
75.0	97.6
77.0	92.9
83.6	122.6

64

TABLE XXIV. SPURIOUS RESPONSE RESULTS AT 76 MEGAHERTZ
FOR VARACTOR-TUNED IC ASSEMBLY

Spurious Order	Spurious Frequency (MHz)	Magnitude Above 1-μV Reference Level (dB)
2	53.000	60.8
3	117.5	70.1
4	58.750	103.5
4	70.25	82.9
5	46.833	114.3
5	91.0	106.4
6	60.666	117.5
6	68.333	106.4
7	51.250	103.0
7	82.166	101.2
8	67.375	111.1
8	103.666	106.8
9	53.900	123.0
9	77.750	85.6
9	83.500	108.2
10	66.8	117.1
10	93.875	123.8
11	75.100	85.6
15	75.357	82.6
22	76.250	80.4
24	75.181	90.6
26	76.206	80.0
28	75.307	89.5

P. MOS INTEGRATED CIRCUITS UNDER RADIATION ENVIRONMENTS

Fundamental studies regarding the behavior of MOS field-effect transistors (FETs) have been carried out by RCA investigators and others since 1964 when it was found that, contrary to belief, MOS transistors can be strongly influenced by a radiation environment. It was previously believed that MOS FETs would be relatively uninfluenced by radiation because the most positively identified radiation effects in semiconductor devices had been associated with minority carrier devices and not with the majority carrier FET device. As a result of these studies, which are surveyed in a recent article, "Designing MOS Systems for Radiation Environments" by A. Holmes-Siedle and K. Zaininger, Solid State Technology, May 1969, pp 40-49 and 71, it has been found that there are two principle effects: the creation of interface states and the introduction of positive charges within the oxide.

It was found that charges trapped in interface states shift the gate threshold toward a positive direction and degrade device performance, i.e., transconductance decreases. Positive charges introduced during irradiation shift the threshold in a negative direction. The direction of these shifts are independent of device type n or p. The magnitude of interface states introduced during irradiation strongly depends on the initial degree of order at the interface that can be controlled by oxidation and annealing techniques prior to irradiation. With present day technologies, this first mechanism can be minimized so that a change in threshold voltage, due to the introduction of positive charges without degradation of device performance, is the major effect of radiation environment.

The quantity of charge introduced in the oxide also depends strongly on the initial degree of order at the interface. However, even with the best oxidation technology, significant shifts in threshold due to this second mechanism are still observed. Other factors that are influential are gate bias and incorporation of a phosphorous doped channel oxide layer. The threshold shifts associated with negative bias under irradiation are typically much less than the shifts under positive bias. MOS p-channel transistors are, therefore, more resistant to radiation effects than n-channel devices, since p-channel transistors are negatively biased under normal operation.

66

MOS transistors are frequently fabricated with two-layer channel oxides, where the top layer is deposited pyrolytically and can be doped as it is put down. A heavy phosphorous doping in this layer has produced resistance to an order of magnitude higher dose level for a given shift in threshold voltage.

Even with the best of present oxide technology, several volts in threshold shift can be expected for p-channel transistors under a radiation flux as high as 10^{16} electron/cm^2. This amount of radiation is typical of space or nuclear environments, barring severe bursts of nuclear energy.

The best success found to date for radiation resistance of insulated gate field-effect transistors has been achieved with devices that were fabricated with aluminum oxide, Al_2O_3, replacing silicon dioxide, SiO_2, as a gate insulator. For an electron fluence up to 1 x 10^{14} electron/cm^2, under either positive or negative bias, only small shifts in threshold bias are detectable. These transistors employ plasma anodized Al_2O_3 as the gate insulator. While various techniques are being explored to obtain Al_2O_3 gate insulators, these films have not been used to date to fabricate MOS integrated circuits.

From a systems point of view, the integrated RF amplifier-mixer should tolerate moderate shifts in threshold voltage. This p-channel MOS IC is made by state-of-the-art oxide technology and by incorporating a layer of phosphorus doped oxide in the channel oxide. A shift in threshold voltage from -1.75 to -3.75 volts can be expected under radiation environments similar to that discussed, but this shift would not be deleterious. In fact, the RF stage would exhibit more power gain with a shift of threshold voltage in the direction described. This occurs since the dual-gate structure of the RF stage is biased by a network such that the device is ON by one threshold voltage above its own threshold. As a result, it would be biased ON harder with the increase in threshold voltage after radiation. There would also be, however, an increase in power dissipation in the RF stage. It is expected that RF stability would still be very good even with the increased gain. The dual-gate device of the mixer stage is biased by a voltage divider network for the first gate and is direct coupled to ground for the second gate. Consequently, these voltages would not change in a radiation environment. The threshold

voltage of the mixer unit, however, would increase under radiation; hence it would not be biased ON as hard. Nevertheless, the conversion gain of the mixer device is not sensitive to this type of variation. With an increase in power dissipation in the RF stage and a decrease in power dissipation in the mixer stage, total power dissipation would remain nearly constant. Overall system gain and sensitivity is likely to improve with a moderate increase in threshold voltage under radiation environment.

For constant gain performance under a radiation environment, the aluminum oxide technology should be applied in the fabrication of the RF amplifier-mixer circuit. However, it is probable that the present MOS circuit would be adequately tolerant to the most likely type of radiation environment.

SECTION III
CONCLUSIONS

An integrated MOS RF amplifier-mixer circuit, capable of receiving signals in the frequency range from 30 to 76 megahertz, was successfully designed and developed. The FM front end exhibited excellent sensitivity, high power gain, good spurious response, cross-modulation, and desensitization performance. The operation of the MOS IC was similar to that of circuits using discrete devices.

The circuit, which consists of seven p-channel MOS enhancement devices fabricated on a common substrate, uses MOS dual-gate devices in both the RF amplifier and mixer stages. The MOS transistors necessary to bias these stages are included on the 30- by 40-mil pellet. The source degeneration resistor-capacitor network of both stages are therefore eliminated. High-frequency-enhancement devices permit the output of the RF amplifier to be direct-coupled to the input of the mixer stage, thus saving an external coupling capacitor and an additional pin in the IC package. For maximum conversion gain the local oscillator was injected at the first gate, and the RF signal at the second gate of the dual-gate mixer.

The RF amplifier-mixer IC was evaluated in a typical military FM receiver at 30 and 76 megahertz. The circuit exhibited a sensitivity of 0.35 and 0.4 of a hard microvolt at 30 and 76 megahertz, respectively, for a 10-dB signal plus noise-to-noise ratio at the audio output. The power gain and dissipation was 34.0 dB and approximately 100 milliwatts, respectively, for a 9-volt supply at both 30 and 76 megahertz. Interfering signal levels, removed by 10 percent from the desired channel frequency, of at least 122 dB above the reference level were required to degrade the 10-dB signal plus noise-to-noise ratio to 6 dB. The circuit met or exceeded contract specifications on sensitivity, power gain, desensitization, and spurious response, except for two spurious frequencies at 76 megahertz.

69

The integrated RF amplifier-mixer was incorporated into a varactor-tuned
assembly and tested over the 63- to 76-megahertz band. The IC front-end
assembly exhibited very good performance, essentially meeting the program
requirements on sensitivity, desensitization, and spurious response.

SECTION IV

RECOMMENDATIONS

The success in developing an integrated RF amplifier-mixer circuit in this program, which essentially met or exceeded all contract specifications over the 30- to 76-megahertz range, has led RCA to recommend that the following areas be investigated in future programs:

a. A natural extension of the present circuit would be to incorporate an MOS voltage-controlled oscillator (VCO) along with the present RF amplifier and mixer, all on a common substrate. Similar to the technique of direct-coupling the RF amplifier to the mixer stage by using enhancement devices, the VCO could also be DC coupled, thus eliminating the external AC coupling capacitor. However, one problem that might be encountered, with the VCO on the same chip as the RF amplifier and mixer, could be coupling of the oscillator signal to the antenna terminals. More work toward developing a monolithic front end, which includes the VCO, is necessary.

b. It was demonstrated during this program that the integrated circuit exhibited very good operation in a varactor-tuned assembly. It would be advantageous to incorporate varactor-diodes in the IC package. There is some possibility that varactors could be processed with MOS devices on a common substrate. However, a more reasonable approach may be to beam lead the diodes to the MOS pellet. Since there are technical difficulties associated with both techniques currently, a strong effort is required in this area.

c. The RF amplifier-mixer IC appears very attractive for low power-dissipation applications. The IC was operated at levels of 20 milliwatts of power dissipation for a 5-volt supply. In addition,

71

power gains in excess of 30 dB were measured at 36 milliwatts of dissipation (note Table XIV). A more thorough investigation of the present circuit's system performance, i.e., sensitivity, desensitization, and spurious response, is needed.

d. There are strong possibilities that the techniques used to develop the integrated RF amplifier-mixer circuit over the 30- to 76-megahertz band could also be applied to other frequency ranges. More specifically, a program to develop a 225- to 400-megahertz UHF front-end IC would certainly be worthwhile.

e. Finally, the process used to fabricate the p-channel, integrated RF amplifier-mixer was developmental. While this process has been reproduced a number of times, and in some ways is similar to an earlier developed n-channel process already in production, there is a need to establish production methods for fabricating p-channel, high-frequency, linear integrated circuits.

DOCUMENT CONTROL DATA - R & D

(Security classification of title, body of abstract and indexing annotation must be entered when the overall report is classified)

1 ORIGINATING ACTIVITY (Corporate author)	2a. REPORT SECURITY CLASSIFICATION
RCA Electronic Components Somerville, New Jersey	Unclassified
	2b. GROUP

3 REPORT TITLE

Linear Integrated Circuits (Field Effect RF Amplifier/Mixer Integrated Circuits)

4 DESCRIPTIVE NOTES *(Type of report and inclusive dates)*

Final Report, 8 April 1968 to 7 April 1969

5 AUTHOR(S) *(First name, middle initial, last name)*

Robert H. Dawson and Stanley Katz

6. REPORT DATE	7a. TOTAL NO. OF PAGES	7b. NO. OF REFS
September 1969	85	3

8a. CONTRACT OR GRANT NO	9a. ORIGINATOR'S REPORT NUMBER(S)
DAAB07-68-C-0301	
b. PROJECT NO. 1H6 62705 A 440	
c. Task 02	9b. OTHER REPORT NO(S) *(Any other numbers that may be assigned this report)*
d.Subtask 18	ECOM-0301-F

10. DISTRIBUTION STATEMENT Each transmittal of this document outside the Department of Defense must have prior approval of CG, US Army Electronics Command, Fort Monmouth N.J. Attn: AMSEL-KL-IC

11. SUPPLEMENTARY NOTES	12. SPONSORING MILITARY ACTIVITY
	United States Army Electronics Command Fort Monmouth, N. J. AMSEL-KL-IC

13. ABSTRACT

An integrated MOS RF amplifier-mixer circuit, capable of receiving FM signals in the 30-to 76-megahertz frequency range, was developed successfully. The front end IC essentially met or surpassed contract specifications on sensitivity, power gain, desensitization, and spurious response. The performance of the integrated-circuit compared favorably to results obtained from circuits using discrete devices.

The circuit, which consists of seven p-channel MOS enhancement devices fabricated on a common substrate, uses MOS dual-gate devices in both the direct-coupled RF amplifier and mixer stages. The MOS transistors necessary to bias these stages are included on the 30-by 40-mil pellet.

The RF amplifier-mixer IC was evaluated in a typical military FM receiver at 30 and 76 megahertz. The circuit exhibited an excellent sensitivity of 0.35 and 0.4 of a hard microvolt at 30 and 76 megahertz, respectively, for a 10-dB signal plus noise-to-noise ratio at the audio output. Power gain and dissipation was 34.0 dB and approximately 100 milliwatts, respectively, for a 9-volt supply at both 30 and 76 megahertz. Desensitization results were very good with interfering signal levels, removed by 10 percent from the desired channel frequency, of at least 122 dB above the reference level required to degrade the 10-dB signal plus noise-to-noise ratio to 6 dB. The integrated RF amplifier-mixer was operated in a varactor-tuned assembly, and performed well over the 63-to 76-megahertz band.

DD FORM NOV 65 **1473**